USING A 3D *IN VITRO* OVARIAN TISSUE CULTURE MODEL TO SCREEN FOR THE FEMALE REPRODUCTIVE TOXICITY OF PHARMACEUTICAL COMPOUNDS

by

Jingshan Xu

Bachelor of Preventive Medicine
Fudan University, 2018

Submitted in Partial Fulfillment of the Requirements

For the Degree of Master of Science in

Environmental Health Sciences

The Norman J. Arnold School of Public Health

University of South Carolina

2020

Accepted by:

Guoshuai Cai, Director of Thesis

Shuo Xiao, Reader

Geoffrey I. Scott, Reader

Cheryl L. Addy, Vice Provost and Dean of the Graduate School

ACKNOWLEDGEMENTS

I am extremely grateful to my deepest appreciation to my committee Dr. Guoshuai Cai, Dr. Shuo Xiao and Dr. Geoffrey I. Scott for their efforts in supporting and guiding me during this research project. I would also like to thank the experts who were involved in the experimental design and data analysis for this research project: Kimberly Maratea from AstraZeneca, Kristin Fabre from Baylor College of Medicine, Dr. Qiang Zhang from Emory University, and Dr. Teresa K. Woodruff from Northwestern University. I am also grateful to thank Jie Zhu and Yaqi Zhang from Northwestern University and Yingzheng Wang from University of South Carolina for their assistance in the follicle culture. I gratefully acknowledge the helpful comments from Alexandra E. Kauffman and Yang Li from University of South Carolina. The financial assistance of the Arnold School of Public Health Start Up Fund at the University of South Carolina, National Institutes of Health (NIH, P01ES028942 and K01ES030014) and National Science Foundation (1832901) to S. Xiao, and NIH UG3ES029073 to TK. Woodruff towards this research is hereby acknowledged.

ABSTRACT

Ovarian toxicity (ovotoxicity) is one of the major side effects of pharmaceutical compounds for women at or before reproductive age. The current gold standard for screening of compounds for ovotoxicity largely relies on preclinical investigations using whole animals. However, *in vivo* models are time-consuming, costly, and harmful to animals. Here, we developed a three-tiered ovotoxicity screening approach starting from encapsulated *in vitro* follicle growth (eIVFG) and screened for the potential ovotoxicity of 8 preclinical compounds from AstraZeneca (AZ). Results from Tier 1 and 2 screenings using eIVFG showed that the first 7 tested AZ compounds, AZ-A, -B, -C, -D, -E, -F, and -G, had no effect on examined mouse follicle and oocyte reproductive outcomes, including follicle survival and development, 17β-estradiol (E2) secretion, ovulation, and oocyte meiotic maturation. However, AZ-H, a preclinical compound targeting the checkpoint kinase 1 (Chk1) inhibitor to potentiate the anticancer effects of DNA-damaging agents, significantly promoted granulosa cell apoptosis and the entire growing follicle atresia at clinically-relevant concentrations of 1 and 10 μM. The more targeted explorations in Tier 2 revealed that the ovotoxic effect of AZ-H primarily resulted from Chk1 inhibition in granulosa cells. Using *in vivo* animal models, the Tier 3 screening confirmed the *in vitro* ovotoxicities of AZ-H discovered in Tiers 1 and 2. Using *in vivo* mouse model, the Tier 3 screening confirmed the in vitro ovotoxicities of AZ-H discovered in Tiers 1 and 2. Also, although AZ-H at 0.1 μM alone was not ovotoxic, it significantly exacerbated gemcitabine-induced ovotoxicities on growing follicles. Taken

together, this study demonstrates that the tiered ovotoxicity screening approach starting from eIVFG identifies and prioritizes chemicals of high ovotoxicity concern.

TABLE OF CONTENTS

LIST OF TABLES

LIST OF FIGURES

LIST OF ABBREVIATIONS

3D..... Three-Dimensional

ATM..... Ataxia Telangiectasia-Mutated

ATR..... ATM and Rad3-Related

AZ..... AstraZeneca

BMP15..... Bone Morphogenetic Protein 15

BSA..... Bovine Serum Albumin

Chk1..... Checkpoint Kinase 1

Chk2..... Checkpoint Kinase 2

DMSO..... Dimethyl Sulfoxide

DOX..... Doxorubicin

eIVFG..... Encapsulated *in Vitro* Follicle Growth

E2..... 17β-Estradiol

EGF..... Epidermal Growth Factor

FBS..... Fetal Bovine Serum

FDA..... Food and Drug Administration

GDF9..... Growth Differentiation Factor 9

GEM..... Gemcitabine

GV..... Germinal Vesicle

GVBD..... Germinal Vesicle Breakdown

H&E..... Hematoxylin and Eosin

hCG..... Human Chorionic Gonadotropin

IACUC ..... Institutional Animal Care and Use Committee

ITS ..... Insulin Transferrin and Selenium

LC_{50} ..... Lethal Concentration 50

MII ..... Metaphase II

min ..... Minute

MTA ..... Material Transfer Agreement

NIH ..... National Institutes of Health

Ovotoxicity ..... Ovarian Toxicity

PFA ..... Paraformaldehyde

PBS ..... Phosphate-Buffered Saline

POF ..... Premature Ovarian Failure

R&D ..... Research and Development

rFSH ..... Recombinant Follicle-Stimulating Hormone

CHAPTER 1

INTRODUCTION

The research and development (R&D) of new drugs is an extremely complex and expensive process. On average, it costs about $2.6 billion and more than 10 years for a new drug to be developed from its initial discovery to marketing approval (DiMasi et al., 2016). Of all the candidate compounds, approximately only 0.1% of them are able to pass preclinical evaluations for clinical trials, and 0.01-0.02% of them will receive final approval from the Food and Drug Administration (FDA) (Bakke et al., 1995; Eisenstein et al., 2005; Wong et al., 2019). Of all the failed compounds, more than 50% of them exhibit unintended toxicities to the tested cells, animals, and healthy volunteers or patients (Waring et al., 2015). Furthermore, post-market safety monitoring results in a withdrawal of 1 - 4% of all marketed drugs for safety concerns (Bakke et al., 1995; Onakpoya et al., 2016; Siramshetty et al., 2016; Wysowski & Swartz, 2005). Female reproductive toxicity is one of the major side effects of pharmaceutical compounds, particularly for the childhood, adolescent, and young adult populations, who are within or will be in reproductive age. However, the majority of recruited healthy volunteers or patients in clinical trials are adult males to protect the limited ovarian reserve and also avoid potential pregnancy in females (Gynecologists, 2015), so the evaluation of potential side effects of different compounds on female reproductive system relies largely on preclinical investigations using whole animals.

The ovary is the primary female reproductive organ and functions to synthesize and secrete sex steroid hormones and to mature and ovulate germ cell oocyte for fertilization and pregnancy. Increasing evidence demonstrates that a broad spectrum of pharmaceutical compounds and environmental chemicals can result in female ovarian toxicity (ovotoxicity) and increase women's risks of premature ovarian failure (POF), hormonal imbalance, and sub- or in-fertility (Bhattacharya & Keating, 2012; Vabre et al., 2017). In contrast to other organ systems in which toxic chemical exposure typically causes subclinical phenotypes or development of overt diseases, predicting the impact of chemicals on the ovary is difficult and can be overlooked for an extended period of time until attempts are made to conceive, or the genetic or epigenetic defects of gametes are discovered in subsequent generation(s).

Thus far, the lack of optimal *in vitro* models makes the gold standard for preclinical testing of the ovotoxicity of chemicals rely primarily on whole laboratory animals. However, *in vivo* models are time- and effort-consuming and costly, and it is also unethical to sacrifice a large number of animals for human benefits. Moreover, the U.S. FDA guideline using whole animals to detect female reproductive toxicity of pharmaceuticals requires examining the estrous cycle and litter size as well as some overt disease phenotypes such as miscarriage, teratogenicity, and infertility (FDA, 2017). However, the specific upstream reproductive endpoints in the ovary, such as follicle development, hormone secretion, and oocyte maturation and ovulation, are equally important, yet difficult to monitor in real time without dissecting whole animals. Ovarian cell lines including both follicular somatic cells (e.g. granulosa cell lines) and denuded oocytes have been cultured *in vitro* for testing chemicals' ovotoxicity (Havelock et al.,

2004; Pocar et al., 2003, 2001). For example, the SV40 transformed cell lines, granulosa cell lines, are used for studying the molecular events regulating granulosa cell steroidogenesis, including expressing follicle stimulating hormone receptors (Keren-Tal et al., 1993). However, the three-dimensional (3D) cell/tissue specific architecture is missing in these cultures. More importantly, normal follicle development and oocyte maturation require orchestrated bidirectional communications between somatic cells and their enclosed oocyte (Biggers et al., 1967; Buccione et al., 1990; Eppig et al., 2005; Gui & Joyce, 2005; Su et al., 2008). For example, the granulosa cells transfer metabolic products such as amino acids, pyruvate, and cholesterol to oocytes through gap junctions to promote oocyte maturation (Biggers et al., 1967; Eppig et al., 2005; Su et al., 2008); in turn, the oocyte-secreted factors such as growth differentiation factor 9 (GDF9) and bone morphogenetic protein 15 (BMP15) control granulosa cell metabolism and differentiation (Buccione et al., 1990; Gui & Joyce, 2005). These facts indicate that for the lack of physical contacts and biochemical crosstalks between somatic cells and oocytes (Chen et al., 2013; Gilchrist et al., 2006; Matzuk et al., 2002; Su et al., 2009; Sugiura et al., 2005), the traditional cultures of individual type of ovarian cells cannot reconstitute the physiology necessary for testing the ovitoxicity of chemical exposure as with intact ovaries or follicles *in vivo*.

The method of in vitro ovarian follicle culture has been used for examining the effect of xenobiotic exposures on female ovarian function, suggesting a robust model for in vitro ovotoxicity testing (Rasmussen et al., 2017; Stefansdottir et al. 2014; Wang et al., 2018; Xiao, Zhang, et al., 2017a; Zhou & Flaws, 2017; Zhou et al., 2015; Zhou & Shikanov, 2018). In our previous studies, we have used the alginate hydrogel

encapsulation method to culture both mouse and human preantral follicles *in vitro* (Xiao, Duncan, et al., 2015; Xiao, Zhang, et al., 2015; Xiao, Zhang, et al., 2017b), which is termed encapsulated *in vitro* follicle growth (eIVFG). The eIVFG maintains the 3D architecture of follicles and recapitulates most of key events of folliculogenesis and oogenesis *in vivo*, including follicle growth and development from the primary or secondary stage to antral stage for maturation, hormone secretion, and oocyte maturation and ovulation (Table 1.1). In the present study, we further developed a novel tiered ovotoxicity screening approach starting from eIVFG and screened for the potential ovotoxicity of 8 preclinical compounds from AstraZeneca (AZ). The *in vivo* or clinically relevant exposure concentrations were used, which were determined based on the *in vivo* pharmacokinetic data in various species (e.g. mouse, rat, and dog) from AZ or previously published results. In summary, our results indicate that the tiered ovotoxicity screening approach allows us to identify and prioritize chemicals of high ovotoxicity concern for more targeted, sophisticated, and mechanistic evaluations.

Table 1.1 The eIVFG maintains the 3D architecture of follicles and recapitulates most of key events of folliculogenesis and oogenesis *in vivo*

***In vivo* model**		**eIVFG**
Folliculogenesis and oogenesis	Follicle growth and development from the primary or secondary stage antral stage for maturation	Follicle grows when maintains architecture and the spatial relationship of the oocyte and its supporting somatic cells (Kreeger et al., 2006; Xiao, Duncan, et al., 2015; Xiao, Zhang, et al., 2015; Xu, Barrett, et al., 2009; Xu et al., 2006).
	Ovulation	During *in vitro* maturation, hydrogel-encapsulated follicles develop mature oocytes within the capacity for fertilization which is similar to that of oocytes matured *in vivo.* (Kreeger et al., 2006; Xiao, Duncan, et al., 2015; Xiao, Zhang, et al., 2015; Xu et al., 2006).
	Gonadotropin regulation	Gonadotropin supplement with adequate concentration is performed to support the hormonal and environmental needs of the follicle culture (Kreeger et al., 2005; Xu et al., 2011).
Steroidogenesis	Hormone secretion: estradiol, androstenedione, and progesterone	The hormone secretion patterns are similar to *in vivo* model (Kreeger et al., 2006; Songsasen et al., 2011; Xiao, Duncan, et al., 2015; Xiao, Zhang, et al., 2015; Xu et al., 2011; Xu, Barrett, et al., 2009; Xu et al., 2006; Xu, West-Farrell, et al., 2009).
Fertilization		Oocytes undergo successful *in vitro* fertilization, and produce implantable zygotes that develop into viable, fertile offspring. Nevertheless, *in vitro*–cultured oocytes which were successfully fertilized is fewer than *in* vivo oocytes (Xu et al., 2006).
Implantation of embryos		Embryos derived from cultured oocytes fertilized *in vitro* and transferred to pseudopregnant female mice were viable (Xu et al., 2006).
Live birth outcomes		Mice derived from oocytes cultured *in vitro* developed normally. Both male and female offspring were fertile. But the live birth rate remains low in the mouse (Xu et al., 2006).

CHAPTER 2

METHODS

Methodologies used for identifying pharmaceutical compounds with high ovotoxicity concern, including materials for lab experiments, and all statistical analyses performed in the study are outlined in the Chapter 2.

2.1 Animals

The CD-1 mouse breeding colony (Charles River Laboratory, Wilmington, MA) was maintained in the animal facility at the University of South Carolina. All mice were housed in polypropylene cages and provided with food and water *ad libitum*. Animals were kept on a 12-hour light/dark cycle (7:00 AM to 7:00 PM) at 23±1°C with 30-50% relative humidity. All methods used in this study were approved by the University of South Carolina Institutional Animal Care and Use Committee (IACUC) and corresponded to the National Institutes of Health (NIH) guidelines and public law.

2.2 Follicle isolation, encapsulation, and culture

Immature ovarian follicles at multilayered secondary stage (150-180 μm, type 5b) were mechanically isolated from 15- or 16-day-old CD-1 female mice as we previously described (Xiao, Duncan, et al., 2015; Xiao, Zhang, et al., 2017a). Only follicles that displayed intact morphology were selected for encapsulation and culture. Selected follicles were encapsulated individually in 0.5% alginate hydrogel (Sigma-Aldrich, St. Louis, MO, USA). Follicles were placed in maintenance media containing minimal essential medium (αMEM with Glutamax, Gibco, Thermo Fisher Scientific Inc.,

Waltham, MA, USA) and 1% fetal bovine serum (FBS, Sigma-Aldrich) for 0.5 hour (hr) after encapsulation. Encapsulated follicles were then individually placed in 96-well plates, with each well containing 100 µl growth media (50% αMEM with Glutamax and 50% Nutrient Mixture [F-12 with Glutamax, Gibco, Thermo Fisher Scientific Inc.] supplemented with 3 mg/ml bovine serum albumin [BSA, Thermo Fisher Scientific Inc.], 20 mIU/ml recombinant follicle-stimulating hormone [rFSH, A. F. Parlow, National Hormone and Peptide Program, National Institute of Diabetes and Digestive and Kidney Diseases, Bethesda, MD, USA], 1 mg/ml bovine fetuin [Sigma-Aldrich], 5 µg/ml insulin, 5 µg/ml transferrin, and 5 ng/ml selenium [ITS, Sigma-Aldrich]). Follicles were cultured at 37°C in 5% CO_2 for 8 days and half of the growth media (50 µl) was replaced every other day. For all experiments, follicles were randomly distributed to experimental groups with each group having 8-12 follicles and 3-5 replicates were performed.

2.3 Follicle growth and survival assessment

Follicles cultured using eIVFG were imaged at each media change using an Olympus CKX53 Inverted Microscope with 10x and 20x objectives (Olympus Corporation, Hachioji-shi, Tokyo, Japan). Follicles were considered dead if they had unhealthy appearing oocytes and/or granulosa cells, or if the integrity of the oocyte and somatic cell interface was visibly compromised. Follicle growth curves were obtained by plotting the average follicle diameter, which was calculated by averaging two perpendicular measurements from basement membrane to basement membrane of each follicle using ImageJ software (National Institutes of Health, Bethesda, MD, USA). Follicle survival rate was calculated by dividing the number of survived follicles on days 0, 2, 4, 6, and 8 to the number of cultured follicles on day 0. For each experimental

group, the follicle growth curve and survival rates on days 0, 2, 4, 6, 8 were plotted, and the lethal concentration 50 (LC_{50}) on *in vitro* cultured follicles was calculated using global nonlinear regression (dose-response curve) which is a four-parameter logistic function via GraphPad Prism (GraphPad Software, San Diego, CA, USA).

2.4 Hormone measurements

The 17β-estradiol (E2) concentrations in the conditioned follicle culture media on day 8 of eIVFG were collected and measured using ELISA kits (Calbiotech, Spring Valley, CA, USA) according to the manufacturer's instructions. Briefly, the anti-estradiol capture antibodies pre-coated wells were incubated with E2 standards, conditioned follicle culture media, and Estradiol Biotin Reagent for 45 minutes (min). Next, the Estradiol Enzyme Reagent was added and incubated for another 45 min. After washing the wells with the washing buffer for three times, the solution of TMB reagent was added and incubated at room temperature for 20 min, resulting in the development of blue color. Last, the reaction was stopped by the addition of Stop Solution and the absorbance was measured using a BioTek Synergy HT microplate reader (BioTek Instruments, Inc., Winooski, VT, USA) at 450 nm within 15 min. All assays were run in duplicate.

2.5 *In vitro* ovulation, oocyte maturation, and oocyte size measurement

On day 8 of eIVFG, follicles were mechanically removed from alginate beads and then incubated in *in vitro* maturation media (αMEM with 10% FBS, 1.5 IU/ml human chorionic gonadotropin [hCG, Sigma-Aldrich], and 10 ng/ml epidermal growth factor [EGF; from R&D Systems, Minneapolis, MN, USA]) for 16 hr at 37°C in 5% CO_2 in air. Oocytes were denuded from surrounding cumulus cells using 0.3% hyaluronidase (Sigma-Aldrich). Oocytes were considered to be arrested at prophase I in the germinal

vesicle (GV) stage if the nucleus was intact, and were considered to have undergone germinal vesicle breakdown (GVBD) if the nucleus was not visible. If a polar body was present in the perivitelline space, the oocytes were classified as metaphase II (MII). Fragmented or shrunken oocytes were classified as degenerated (D). For all MII oocytes, the oocyte diameter was obtained from two perpendicular measurements, including the zona pellucida. The first measurement detected the widest diameter of oocyte and the second measurement originated at a right angle from the midpoint of the first measurement. The final oocyte diameter was calculated by averaging the two obtained measurements.

2.6 AZ compound exposure and ovotoxicity testing

All 8 tested pharmaceutical compounds were kindly gifted from AZ (Cambridge, United Kingdom) from projects that closed because of non-female reproductive toxicity safety reasons identified during preclinical or clinical development. Because the Material Transfer Agreement (MTA) with AZ, we named them from AZ-A to AZ-H instead of using their original AZ library IDs. However, for the compounds of AZ-A and AZ-H that are commercially available now for scientific research, we started to use their original AZ library IDs (AZD8542 for AZ-A and AZD7762 for AZ-H) and also introduced their molecular target from the Tier 2 screening. All tested AZ compounds were dissolved in 100% dimethyl sulfoxide (DMSO, Sigma-Aldrich) to make a stock concentration at 200 mM and the stock solutions were stored at -20°C and away from light. For ovotoxicity testing, the stock solutions were diluted to the targeted exposure concentrations in follicle culture media. In Tier 1 ovotoxicity screening, follicles were treated with each tested candidate compound at 10 μM from day 2 to day 8 of eIVFG. We started compound

exposure from day 2 instead day 0 to exclude any dead follicles within the first 2 days of eIVFG that might have resulted from mechanical manipulation during follicle isolation. In Tier 2 ovotoxicity screening, follicles were treated with AZ-A as the negative control and AZ-H as the positive control at 0, 0.1, 1, and 10 μM for 24 hours from day 2 of eIVFG, followed by a continuous culture without AZ compound until day 8 of eIVFG. The rationale for determining *in vitro* compound exposure concentrations was described in the Results section. For both Tier 1 and Tier 2 screenings, the assessments of follicle and oocyte reproductive outcomes were performed as described above, including follicle survival, follicle development, E2 secretion, and *in vitro* ovulation and oocyte maturation.

2.7 Chk1 or Chk2 inhibitor treatment and ovotoxicity testing

Another set of multilayered secondary follicles were isolated and cultured using eIVFG. Follicles were treated with three specific Chk1 inhibitors, including Rabusertib at 2 μM, CHIR-124 at 0.2 μM, and MK-8776 at 20 μM, and one Chk2 inhibitor, BML-277 at 5 μM from day 2 to day 8 of eIVFG. The follicle survival and development were examined as described above. The concentrations we used were either based on human plasma/serum levels in clinical trials or based on previous results that showed effective checkpoint kinase inhibition in *in vitro* cultured cell lines. The detailed justification was described in the Results section.

2.8 *In vivo* animal exposure

In order to investigate whether the gained ovotoxicities of AZ-H in Tier 1 and 2 screenings could be validated using *in vivo* animal models, 21-day-old CD-1 female mice were intraperitoneally injected with 25 mg/kg of AZ-H dissolved in 50 μl DMSO. We

used 21-day-old mice because their ovaries contain all developmental stages of preantral and antral follicles, indicating a good *in vivo* animal model to study the impact of xenobiotic exposure on female ovarian functions (Y. Wang et al., 2019a; Y. Wang et al., 2018). The same volume of DMSO was used as the vehicle control. AZ-A that showed negative ovotoxicity in Tiers 1 and 2 screenings was used as negative control and the exposure dose of AZ-A was at 20 mg/kg through intraperitoneal injection. The rationale of the *in vivo* dose selection for both AZ-A and AZ-H was described in the Results section. Ovaries were collected 24 hr post-injection for histology and TUNEL staining.

2.9 Gemcitabine and doxorubicin treatment

Follicles were treated with different concentrations of gemcitabine (GEM, Sigma-Aldrich) at 0, 0.02, 0.1, and 0.5 μM and doxorubicin (DOX, Sigma-Aldrich) at 0, 10, 20, and 50 nM alone or with AZ-H at 0.1 μM for 24 hr, followed by a continuous culture using compound-free growth media until day 8 of eIVFG. The follicle and oocyte reproductive outcomes were assessed as described above, including follicle survival and follicle development. The specific rationale of using GEM and DOX for co-treatment experiments and determination of concentration range were described in the Results section.

2.10 Histology and TUNEL assay

For *in vitro* exposure experiments, follicles were collected at 24 hr after vehicle or AZ compound treatment and fixed overnight at 4°C in 4% PFA-Cacodylate-Ca^{2+} Fixation Buffer (4% paraformaldehyde [PFA; Sigma-Aldrich], 0.1 M Sodium Cacodylate [Electron Microscopy Sciences, Hatfield, PA, USA], 0.1 M Sucrose [Sigma-Aldrich], 10 mM Calcium chloride [$CaCl_2$; Thermo Fisher Scientific Inc.], pH=7.4). After washing

with 1× phosphate-buffered saline (PBS, Thermo Fisher Scientific Inc.) three times, fixed follicles were dehydrated in ascending concentrations of ethanol (50%-100%) and embedded in paraffin (Sigma-Aldrich). For *in vivo* exposure experiments, ovaries were collected 24 hr after vehicle or AZ compound injection, fixed in Shandon™ Formal-Fixx™ 10% Neutral Buffered Formalin solution (ThermoFisher Scientific Inc.) for 24 hr, and embedded in paraffin. Both embedded follicles and ovaries were sectioned at the thickness of 5 μm with a RM 2165 microtome (Leica Microsystems, Nussloch, Germany). For histology staining, paraffin sections of follicles or ovaries were stained with hematoxylin and eosin (H&E, Thermo Fisher Scientific Inc.) as we previously described (Xiao, Duncan, et al., 2015). The DeadEnd™ Fluorometric TUNEL System Kit (Promega, Madison, WI, USA) was used to detect apoptotic cells according to the manufacturer's instructions. Briefly, paraffin sections of follicles or ovaries were deparaffinized, rehydrated, and fixed in 4% formaldehyde in 1× PBS. After permeabilizing by 20 μg/ml Proteinase K solution for 10 min, the TdT reaction mix was added to the ovarian/follicular sections and incubated for 1 hr at 37°C in a humidified chamber. The sections were counter-stained using Vectashield Mounting Medium with DAPI (Vector Laboratories, Burlingame, CA, USA) and TUNEL positive signals were analyzed under Olympus BX51 microscope (Olympus Corporation, Hachioji-shi, Tokyo, Japan) and quantified by ImageJ software. The relative TUNEL fluorescence intensity was calculated according to the following formula: intensity = total TUNEL positive signal pixel intensity / area.

2.11 Statistical analyses

Follicle growth, survival, hormone secretion, and oocyte reproductive outcomes were analyzed from 3 independent cultures in which 8-12 follicles were included in each experimental group and replicate. Follicle growth pattern and survival rates on the same day, hormone secretion on day 8, ovulated MII oocyte percentage and diameter, and TUNEL positive signal in different drug-treated groups were analyzed using one-way ANOVA. The post hoc test was performed to compare the difference between two groups if a significant difference was observed. The significance level was set at $P < 0.05$.

CHAPTER 3

RESULTS

3.1 The development of a tiered ovotoxicity screening

To efficiently and effectively identify and prioritize pharmaceutical compounds of high ovotoxicity concerns for more advanced assessments, we developed a tiered ovotoxicity screening starting from eIVFG (Figure 3.1). In Tier 1, follicles were treated with each candidate compound at a single high dose from day 2 to day 8 of eIVFG. During the entire compound exposure window, the follicle and oocyte reproductive outcomes were evaluated, including follicle survival, follicle growth and development, sex steroid hormone secretion, and *in vitro* ovulation and oocyte maturation. If no ovotoxic outcome was discovered, the tested compound would be identified as having no ovotoxicity concern. In contrast, if any adverse readouts were detected, the candidate compound would be considered as a suspect ovotoxic chemical and advanced to Tier 2 screening with more sophisticated testing, such as the dose-response expsoure, specific window exposure, or more in-depth cellular or molecular targeted toxicity investigations. The specific experimental design in Tier 2 was dependant on the ovotoxicity results obtained in Tier 1. For compounds that exhibited negative ovotoxic outcomes in Tier 2, they would be reconsidered as low ovotoxicity concern. However, if the tested compounds showed consistent ovotoxicities between Tier 1 and 2, we would further advance them to Tier 3 screening with *in vivo* animal exposure and toxicity validation. If a tested compound shows consistent ovotoxicities in all three tiers, it was identified as an

ovotoxic chemical. If a compound showed inconsistent ovotoxicities between *in vitro* and *in vivo* models, more factors would be considered and investigated, such as liver metabolism, pharmacokinetics/toxicokinetics, local or systemic effects.

3.2 Effects of AZ compounds on follicle survival, development, and hormone secretion in Tier 1 screening

We used 8 AZ compounds (AZ-A to AZ-H) to test the performance of the developed tiered ovotoxicity screening as described in Figure 3.1. Based on our internal pharmacokinetic results in various species and published data, the majority of tested compounds had the maximum plasma or serum concentrations up to 10 μM. In the Tier 1 screening, we therefore treated cultured follicles with each candidate compound at a high concentration at 10 μM from day 2 to day 8 of eIVFG. In the control group, the alginate hydrogel encapsulation maintained the 3D architecture of cultured follicles and supported follicle growth from multilayered secondary stage on day 0 to antral stage on day 8 during eIVFG (Figure 3.2A). The follicle diameter increased from 161.9 ± 15.3 μm on day 0 to 405.4 ± 28.4 μm on day 8, and the follicle survival rate was 100% on day 8 (Figure 3.2A). Follicles treated with all 8 AZ compounds at 10 μM except AZ-H showed comparable follicle survival rates and growth patterns to the control group (Figure 3.2A and 2B). However, follicles treated with AZ-H at 10 μM resulted in 100% follicle death starting from day 4 of eIVFG (Figure 3.2A-2C).

To investigate the effects of AZ compounds on ovarian steroidogenesis, we collected conditioned follicle culture media on day 8 and measured the concentration of E2, an important sex steroid hormone synthesized and secreted from growing follicles that supports the functions of ovary/follicles, downstream reproductive organs, and

systemic health (Buyuk et al., 2010). ELISA results indicated that there were no significant difference in the E2 secretion levels between control group and follicles treated with all tested AZ compounds except AZ-H (Figure 3.3). The extremely low concentrations of E2 in AZ-H treatment group reflected the above findings that all treated follicles were dead on day 8. These results indicated that there was a low ovotoxicity concern for the AZ compounds of AZ-A, AZ-B, AZ-C, AZ-D, AZ-E, AZ-F, and AZ-G. However, AZ-H had suspected ovotoxicity and requires further investigations.

3.3 Effects of AZ compounds on follicle ovulation and oocyte meiotic maturation in Tier 1 screening

We next treated grown antral follicles with hCG on day 8 to determine the effect of AZ compound exposure during folliculogenesis and oogenesis on follicle ovulation and oocyte meiotic maturation. Results showed that 88.9 ± 0.2% of antral follicles in the control group ruptured and ovulated MII oocytes with the first polar body extrusion (Figure 3.4A and 4B). The ovulated MII oocytes had normal morphological appearance and the average MII oocyte diameter was 89.4 ± 3.5 μm (Figure 3.4C). Because there was 100% of follicle death on day 8 after AZ-H treatment (Figure 3.2), no follicle was collected for *in vitro* ovulation and oocyte maturation (crosses in Figure 3.4B and 4C). For the follicles treated with all the other 7 AZ-compounds, they had comparable percentage of MII oocytes, morphological appearance, and oocyte size compared to the control group (Figure 3.4), suggesting that these 7 AZ-compounds did not interfere with follicle ovulation and oocyte meiotic maturation.

3.4 Effects of AZ-H on follicle survival and development in Tier 2 screening

Based on the ovotoxicity screening results in Tier 1, we next selected the ovotoxic compound AZ-H for a more advanced Tier 2 screening. We also chose AZ-A that did not show ovotoxicity in Tier 1 as the negative control and used DMSO as the vehicle control. AZ-A and AZ-H have the AZ compound library ID as AZD8542 and AZD7762 (so referred to below), respectively. AZD8542 was designed as a hedgehog pathway antagonist to inhibit tumor progression by targeting fibroblasts (Hwang et al., 2012); and AZD7762 was designed as a checkpoint kinase 1 and 2 (Chk1/2) inhibitor to potentiate the therapeutic effect of DNA damaging agents on tumor cells (Zabludoff et al., 2008). Based on the results from previous clinical trials, the maximal plasma concentration of AZD7762 was between 0.83-1.10 μM in humans (Sausville et al., 2014; Seto et al., 2013) and 9 μM in dogs (unpublished data from AZ). Therefore, we performed a dose-response study by treating cultured follicles at 0, 0.1, 1, and 10 μM in Tier 2. We also chose a more specific exposure window by treating follicles for 24 hr because results from Tier 1 indicated that AZD7762 caused remarkable morphological changes to follicles within 24 hr (Figure 3.2C). For the compound of AZD8542, previous studies reported that the *in vitro* treatment of AZD8542 at 0.1-1 μM effectively inhibited the hedgehog pathway in human pancreatic stellate cells 24 hr after compound treatment (Hwang et al., 2012). Therefore, we used the same exposure concentration range and window as the AZD7762.

Consistent to the ovotoxicity screening results in Tier 1, follicles treated with all tested concentrations of AZD8542 had comparable follicle survival rates (Figure 3.5A, left panel), follicle development patterns (Figure 3.5A, right panel), secreted E2 levels (Figure 3.6A), and *in vitro* ovulation and oocyte meiotic division outcomes (Figure 3.6B)

compared to the control group. However, for the follicles treated with AZD7762 at 1 or 10 μM, all follicles were dead on day 4 or day 6 (Figure 3.5B and 5C) and the E2 secretion levels also significantly decreased on day 8 (Figure 3.6A). When follicles were treated with AZD7762 at 0.1 μM, the follicle survival rate and terminal diameter on day 8 decreased by 9.9% and 10.4%, respectively, compared to the control group, but the changes were not statistically significant (Figure 3.5B). At the exposure concentration of 0.1 μM, both the E2 secretion levels and MII oocyte percentages after *in vitro* ovulation were comparable to the control group (Figure 3.6). These results indicated that Tier 1 and Tier 2 screenings had consistent results and AZD7762 exhibits ovotoxicities when the exposure level is at or higher than 1 μM.

3.5 AZD7762 targeted granulosa cells to promote follicle atresia

We next selected the ovotoxic AZD7762 for more targeted histological staining and TUNEL assay. DMSO was used as the vehicle control and AZD8542 was used as the negative control. At 24 hr post-vehicle (DMSO) or 10 μM AZD8542 treatment, follicles had comparable morphology and TUNEL stainings to the control group (Figure 3.7A). However, follicles treated with AZD7762 at 10 μM showed markedly increased granulosa cell apoptosis indicated by the DNA fragmentation in TUNEL staining (Figure 3.7A). Differing from some ovotoxic chemicals such as DOX that damage the outer layers of the theca cells and granulosa cells and then promote the entire follicle atresia (Xiao, Zhang, et al., 2017a), AZD7762 resulted in a greater degree of apoptosis in the inner layers of the granulosa cells (Figure 3.7A). Moreover, up to 24 hr exposure of AZD7762, TUNEL staining results indicated that the central oocytes did not show obvious DNA damage compared to their surrounding somatic cells (Figure 3.7, white

inserts). These data indicated that AZD7762 primarily targets inner granulosa cells to promote the entire follicle atresia.

3.6 The inhibition of Chk1 but not Chk2 resulted in AZD7762-induced ovotoxicities

Since AZD7762 was found to have an equal inhibitory potency for Chk1 and Chk2 (Ma et al., 2011; Morgan et al., 2010; Wang et al., 2018; Zabludoff et al., 2008), we next treated follicles with more specific checkpoint kinase inhibitors to differentiate the role of Chk1 and Chk2 in AZD7762-induced ovotoxicities. The tested inhibitors included Chk1 inhibitors Rabusertib, CHIR-124, and MK-8776, and Chk2 inhibitor, BML-277. The exposure concentrations were determined either based on human plasma/serum levels for the cases of Rabusertib and MK-8776 (Karp et al., 2012; King et al., 2014; Wang et al., 2014; Wehler et al., 2017) or based on previous *in vitro* studies that showed effective checkpoint kinase inhibition in cultured cells for the cases of CHIR-124 and BML-277 (Arienti et al., 2005; Boudny et al., 2019; Dai et al., 2011; Tse et al., 2007; Tuppi et al., 2018). The ovotoxicity screening results revealed that all three tested Chk1 inhibitors exhibited similar ovotoxicities as AZD7762. Specifically, upon the treatment of Rabusertib at 2 μM, CHIR-124 at 0.2 μM and MK-8776 at 20 μM, the follicle survival rates were decreased to 0, 25%, and 4%, respectively, on day 8 of eIVFG (Figure 3.7B and 7C). Interestingly, follicles treated with the specific Chk2 inhibitor BML-277 at 5 μM had comparable follicle survival rates and growth patterns to the control group (Figure 3.7B and 7C). These results suggested that the inhibition of Chk1 but not Chk2 was responsible for the AZD7762-induced ovotoxicities on growing follicles.

3.7 AZD7762 consistently promoted growing follicle atresia *in vivo*

To further validate the ovotoxicities of AZD7762 observed in Tiers 1 and 2 studies, we next performed *in vivo* animal exposure in Tier 3 screening. In previous rodent models, animals were intravenously or intraperitoneally injected with AZD7762 at 10-25 mg/kg, which effectively potentiated chemotherapeutical drug-induced tumor cell death (Itamochi et al., 2014; Ma et al., 2012; Quin et al., 2016; Zabludoff et al., 2008). We therefore treated 21-day-old CD-1 female mice with AZD7762 at 25 mg/kg body weight once. Meanwhile, DMSO was used as the vehicle control and AZD8542 as the negative control. The treatment dose of AZD8542 was at 20 mg/kg which has been demonstrated to significantly inhibit tumor growth in an *in vivo* colon cancer mouse model (Hwang et al., 2012). Both histology and TUNEL staining of ovaries collected 24 hr after vehicle or AZ compounds injection indicated that AZD8542 treated ovaries had similar ovary or follicle morphology and comparable levels of ovarian cell apoptosis compared to the vehicle-treated ovaries (Figure 3.8). However, AZD7762 significantly increased granulosa cell apoptosis in the secondary and antral stages of follicles, which was characterized by the pyknotic and fragmented nuclei in histological staining (Figure 3.8A, black squares) and the DNA-fragmented nuclei in TUNEL staining (Figure 3.8A, white squares). Similar to the *in vitro* ovotoxic patterns (Figure 3.7), *in vivo* results also showed that AZD7762 caused a greater degree of cell apoptosis in the inner layers of the granulosa cells compared to outer cell layers (Figure 3.8A, white squares). With respect to the earlier stage of primordial follicles that we cannot examine using eIVFG, both histological and TUNEL stainig results indicated that there was no significant difference between all treatment groups (Figure 3.8A, red squares). These results indicated that the

obtained ovotoxicities from eIVFG could be validated in *in vivo* animal models, and AZD7762 primarily targeted growing follicles but not primordial follicles to result in ovotoxicities.

3.8 AZD7762 exacerbated ovotoxicity of GEM but not DOX during eIVFG

Since AZD7762 was designed as a Chk1 inhibitor to enhance DNA-damaging agent-induced cancer cell apoptosis (Zabludoff et al., 2008), we next determined whether co-treatment with AZD7762 exacerbated chemodrug-induced ovotoxicities. We chose GEM as the co-treated chemotherapeutic drug because it was used by most of previous studies to test the synergistic anti-cancer effect of AZD7762 (Liu et al., 2017; Morgan et al., 2010; Sausville et al., 2014; Seto et al., 2013; Zabludoff et al., 2008) and GEM has also been reported to cause ovotoxicity by promoting growing follicle atresia (Yuksel et al., 2015). Additionally, we tested the potential enhancing effect of AZD7762 on DOX, another commonly used chemotherapeutic drug showing ovotoxicities on growing follicles (Ben-Aharon et al., 2010; Roti Roti et al., 2012; Wang et al., 2019b; Xiao, Zhang, et al., 2017a). Both GEM and DOX showed dose-dependent ovotoxicities on cultured follicles during eIVFG as we and others previously demonstrated (Figure 3.9A and 9B) (Xiao, Zhang, et al., 2017a; Yuksel et al., 2015). The treatment of AZD7762 at 0.1 μM did not affect follicle development and survival (Figure 3.2); however, it significantly promoted GEM-induced follicle atresia and inhibition of follicle growth and development, particularly when GEM was at or above 0.1 μM (Figure 3.9A). The LC_{50} of GEM on follicle survival was 0.13 μM (Figure 3.9C), however, it significantly decreased to 0.04 μM after follicles were co-treated with 0.1 μM AZD7762 (Figure 3.9C). Interestingly, both the follicle survival rates and follicle terminal diameters were similar

between the DOX only and DOX and AZD7762 co-treatment groups (Figure 3.9B), suggesting that there is no exacerbating effect of AZD7762 on DOX-induced ovotoxicity. Taken together, these results indicated that the co-treatment of AZD7762 could exacerbate chemotherapy-induced ovotoxicity, but the effect depended on the specific anti-cancer agents, which have distinct cell-killing mechanisms.

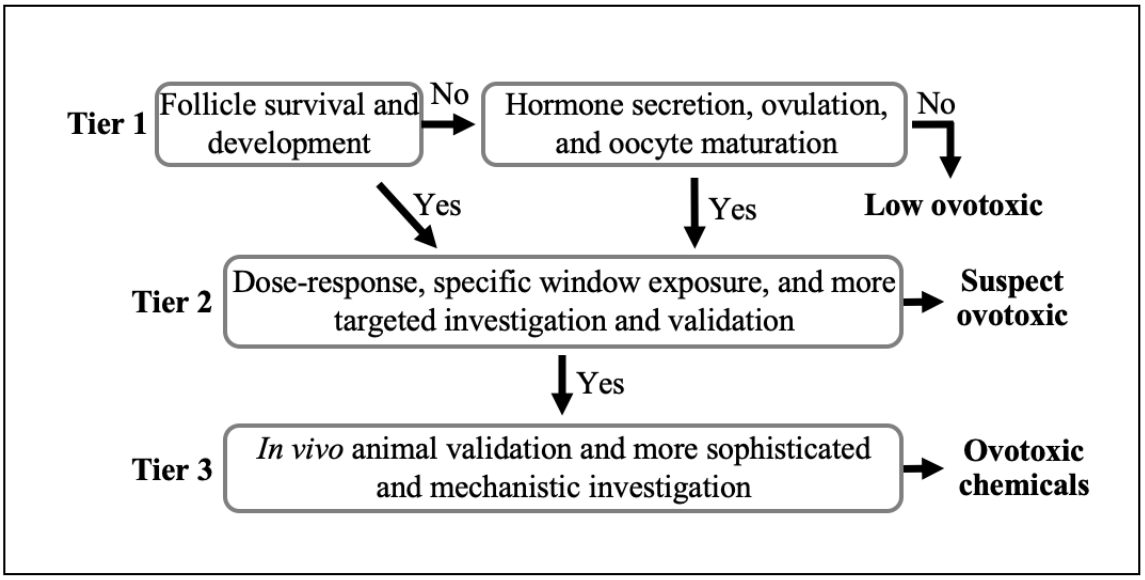

Figure 3.1 The tiered ovotoxicity screening strategy for testing the effect of pharmaceutical compounds on female reproductive health and fertility.

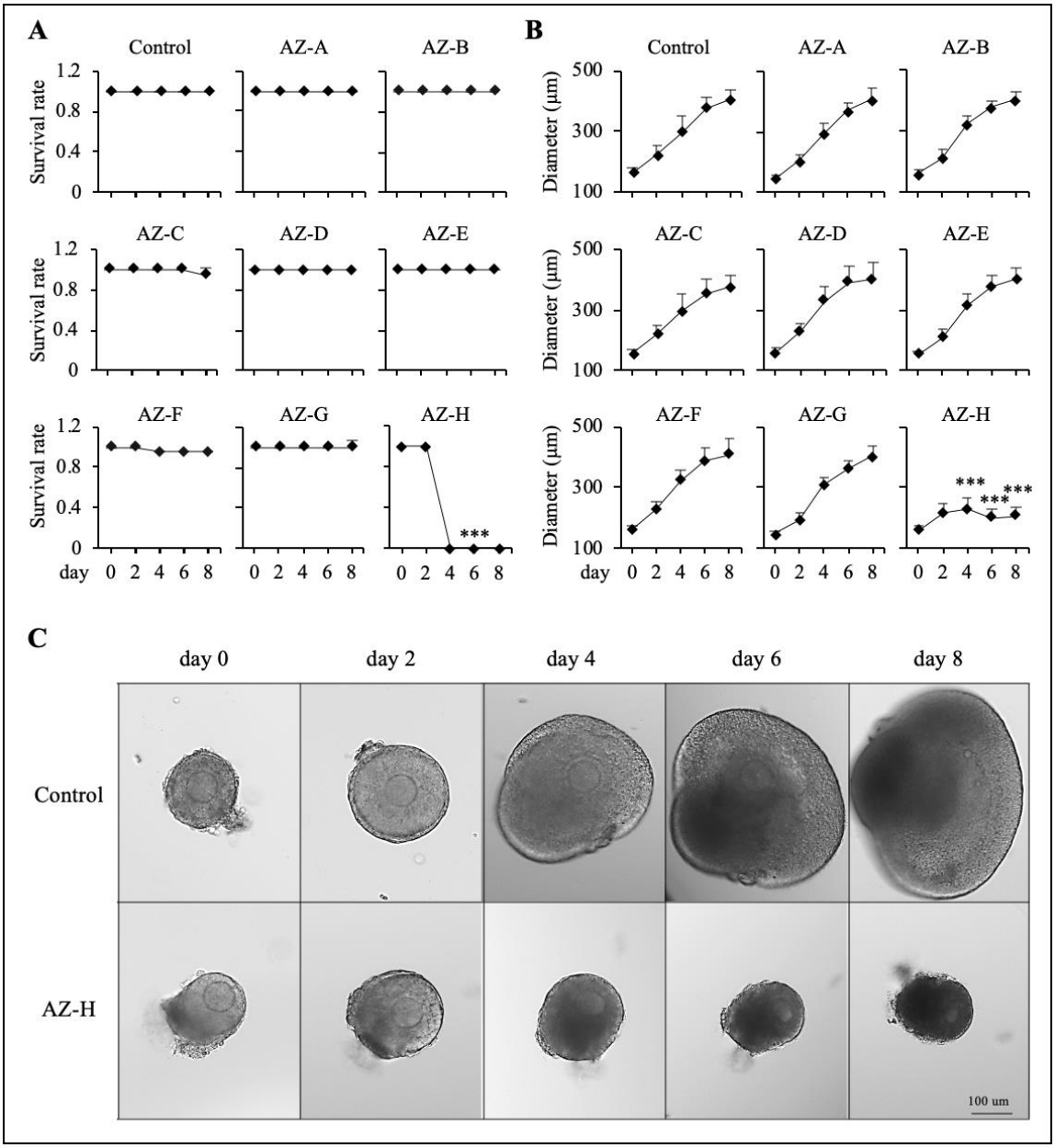

Figure 3.2 Effect of 8 AZ compounds (AZ-A to AZ-H) on follicle survival and development during encapsulated *in vitro* follicle growth (eIVFG). (A-B) Follicle survival rates (A) and follicle diameters (B) during eIVFG after AZ compound exposure at 10 μM from day 2 to day 8. (C) Representative images of follicles during eIVFG treated with vehicle or AZ-H at 10 μM from day 2 to day 8. Error bar: standard deviation; ****p<0.001* compared to control group; scale bar: 100 μm. N=8-12 follicles in each experimental group and three replicates were performed.

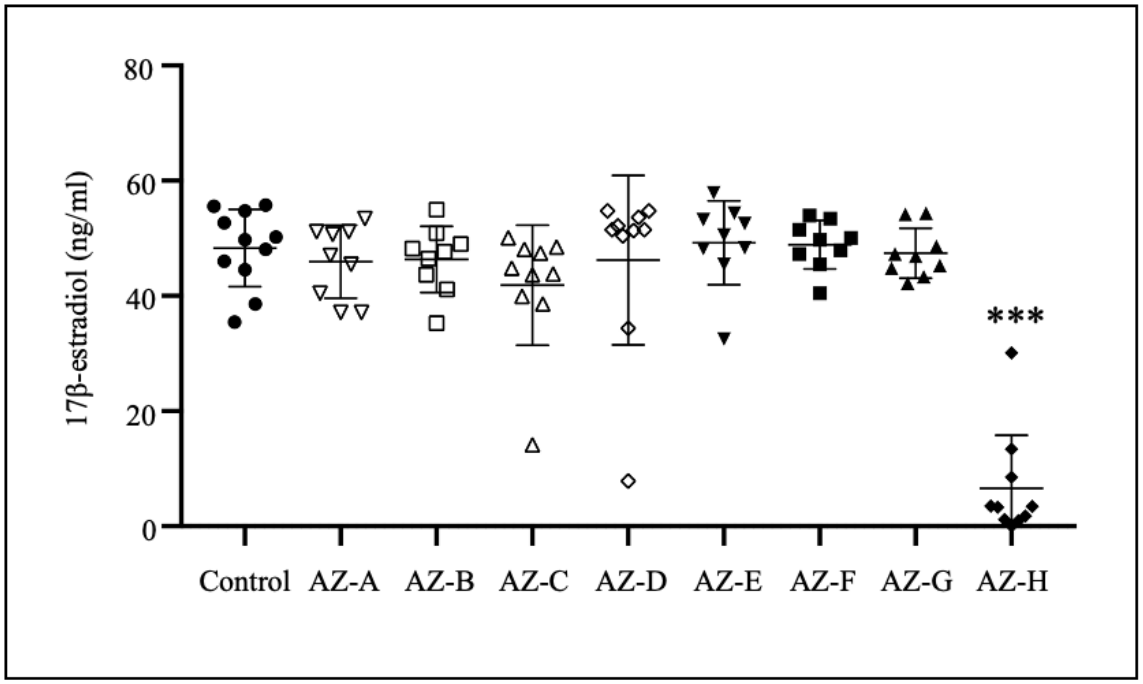

Figure 3.3 Effect of 8 AZ compounds (AZ-A to AZ-H) on 17β-estradiol (E2) secretion on day 8 of eIVFG. Error bar: standard deviation; ****p<0.001* compared to control group. N=8-12 follicles in each experimental group and three replicates were performed.

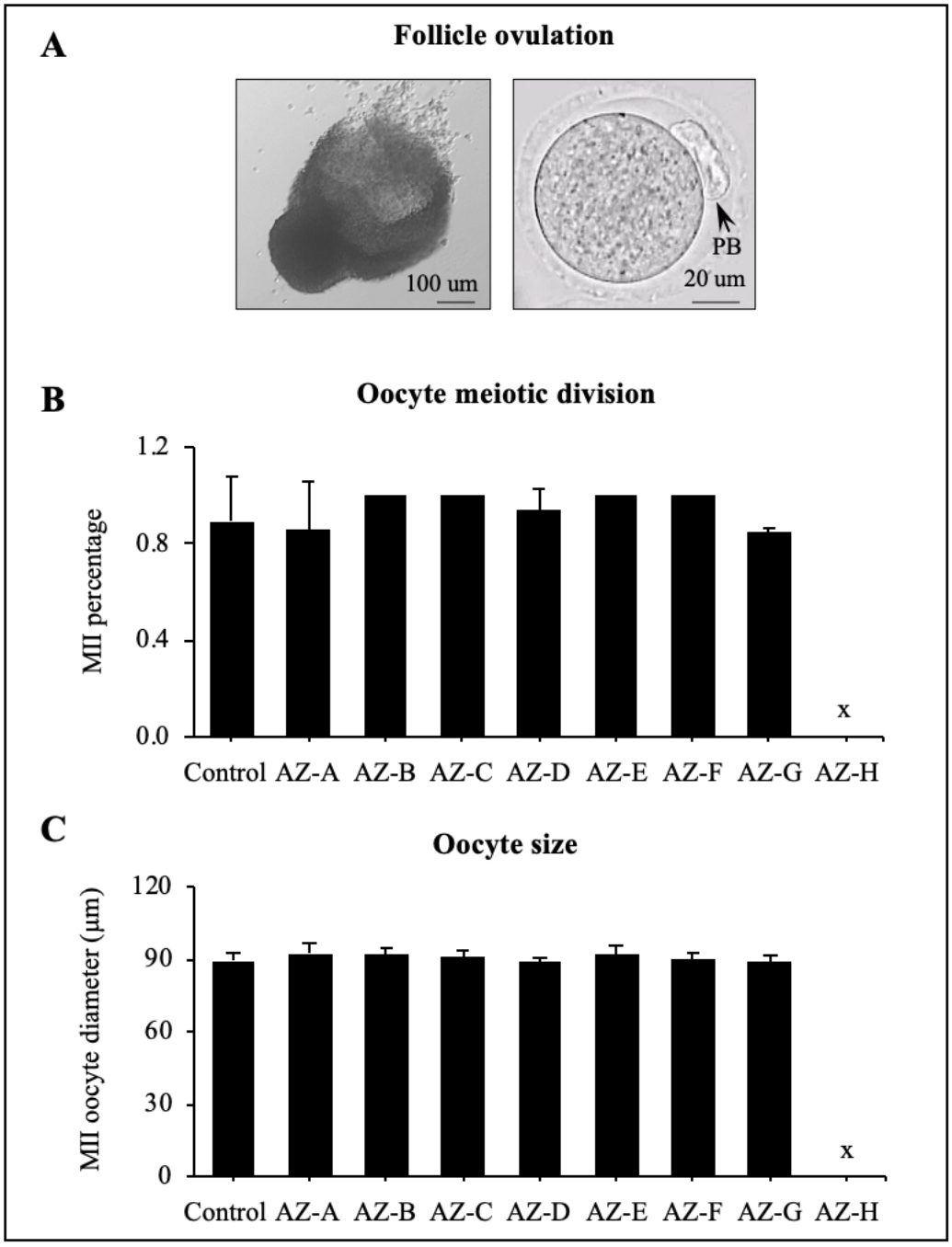

Figure 3.4 Effect of 8 AZ compounds (AZ-A to AZ-H) on *in vitro* ovulation and oocyte meiotic maturation. (A) Representative images of a ruptured follicle (left) and ovulated metaphase II (MII) oocyte (right) after treatment with human chorionic gonadotropin (hCG) for 14 hours. (B-C) Oocyte MII percentages (B) and MII oocyte diameter (C) after *in vitro* ovulation and oocyte maturation. Scale bar: 100 μm for ruptured follicle and 20 μm for MII oocyte; error bar: standard deviation. PB: polar body. The cross marks indicated no follicles were selected for *in vitro* ovulation because of the 100% follicle death upon AZ-H treatment. N=8-12 follicles in each experimental group and three replicates were performed.

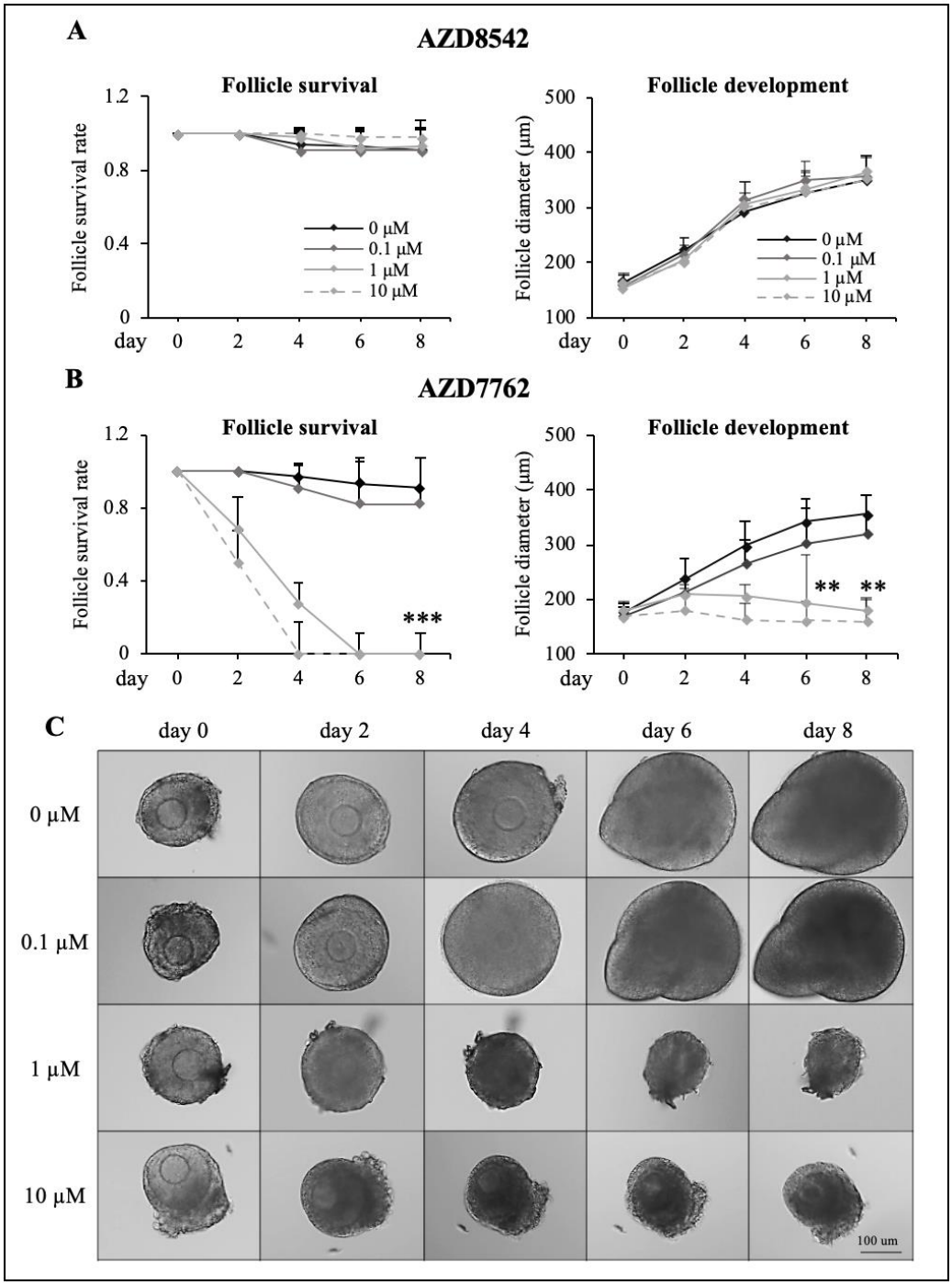

Figure 3.5 Effect of AZD8542 and AZD7762 on follicle survival and development during encapsulated *in vitro* follicle growth (eIVFG). (A-B) Follicle survival rates and follicle diameters during eIVFG upon different concentrations of AZD8542 (A) and AZD7762 (B) treatment. (C) Representative images of follicles during eIVFG treated with AZD7762 at 0, 0.1, 1 and 10 μM for 24 hours (hr). Scale bar: 100 μm; error bar: standard deviation; ***p<0.01*; ****p<0.001* compared to control group. N=8-12 follicles in each experimental group

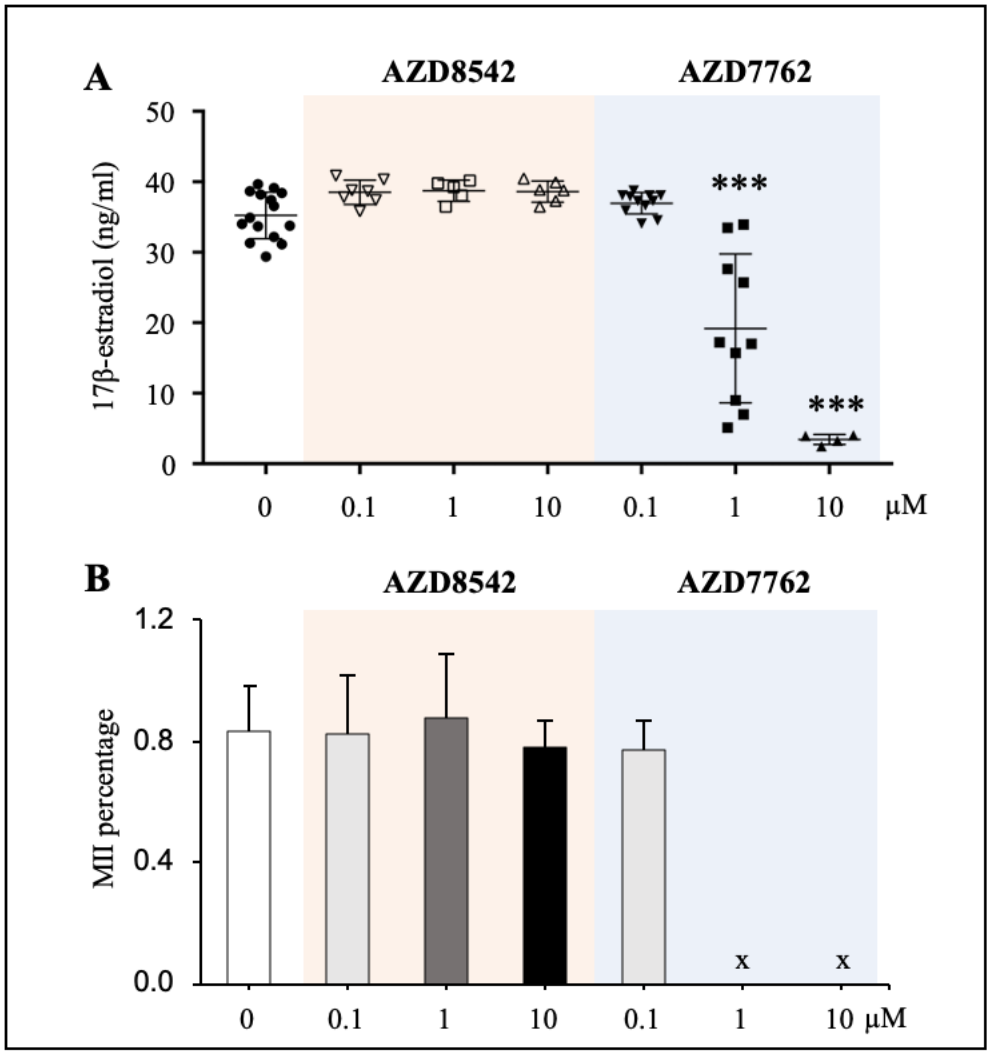

Figure 3.6 Effect of AZD7762 and AZD8542 on 17β-estradiol (E2) secretion and oocyte maturation *in vitro*. (A) E2 secretion levels on day 8 of eIVFG after follicles were treated with different concentrations of AZD8542 and AZD7762 for 24 hr. (B) Oocyte metaphase II (MII) percentages from follicles treated with different concentrations of AZD8542 and AZD7762 for 24 hr. Error bar: standard deviation; ****p<0.001* compared to control group. The cross marks indicated no follicles were selected for *in vitro* ovulation because of the 100% follicle death upon AZ-H treatment. N=8-12 follicles in each experimental group and three replicates were performed.

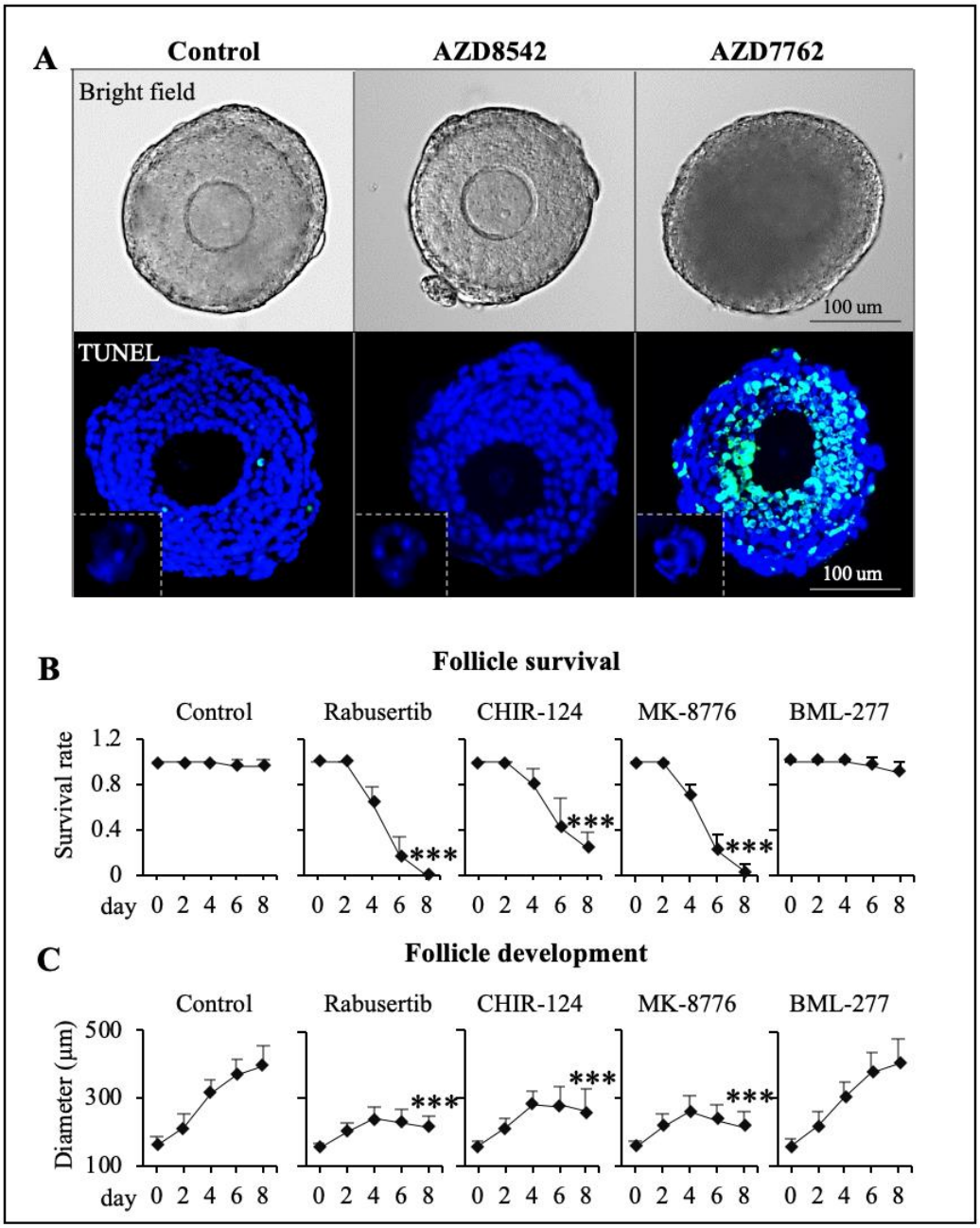

Figure 3.7 Target inhibition of AZD7762 on ovarian follicle. (A) Representative images of follicles in bright field and follicular cell apoptosis after follicles were treated with AZD7762 and AZD8542 exposure at 10 μM for 24 h *in vitro*. Blue: DAPI; green: DNA fragmentation revealed by TUNEL staining. Scale bar: 100 μm. White squares indicated the TUNEL staining of oocytes. N=5-10 follicles for each experimental group and three replicates were performed. (B-C) Effect of three Chk1 inhibitors (Rabusertib at 2 μM, CHIR-124 at 0.2 μM and MK-8776 at 20 μM) and one Chk2 inhibitor (BML-277 at 5 μM) on follicle survival (B) and development (C) during encapsulated *in vitro* follicle growth (eIVFG). Error bar: standard deviation; ****p<0.001* compared to control group. N=8-12 follicles in each experimental group and three replicates were performed.

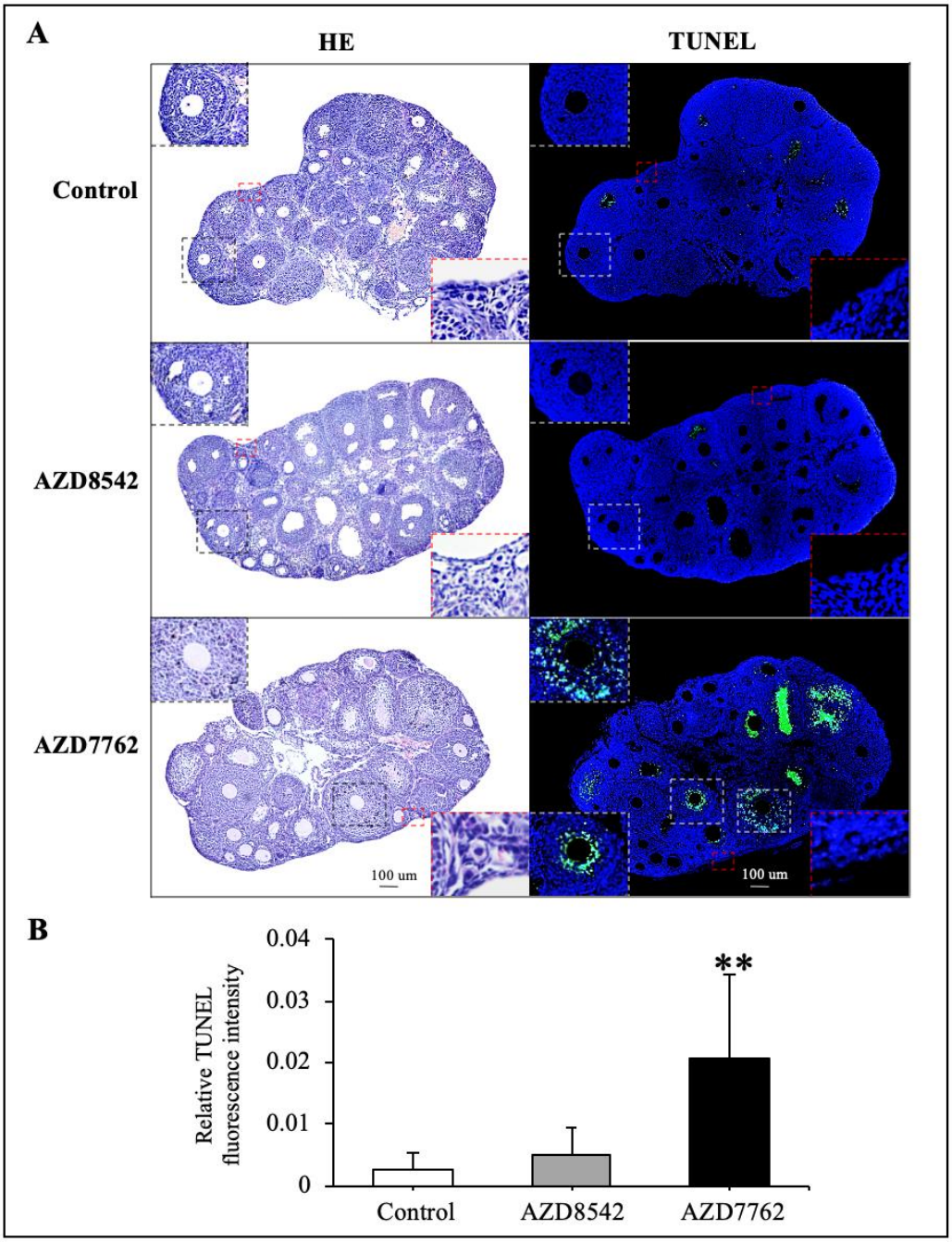

Figure 3.8 Effect of AZD7762 and AZD8542 on ovarian follicle atresia *in vivo*. (A) Representative ovary histological and TUNEL staining images 24 hours (hr) after treatment of vehicle, AZD7762 at 25mg/kg, and AZD8542 at 20mg/kg through intraperitoneal injection. Black squares indicated the histological staining of growing follicles, white squares indicated the TUNEL staining of growing follicles, and red squares indicated the TUNEL staining of primordial follicles. (B) Relative TUNEL fluorescent intensity in the ovaries treated with vehicle, AZD7762, and AZD8542. Scale bar: 100 μm. Error bar: standard deviation; $**p<0.01$. Blue: DAPI; green: DNA fragmentation revealed by TUNEL staining. N=3-7 mice/ovaries in each treatment group.

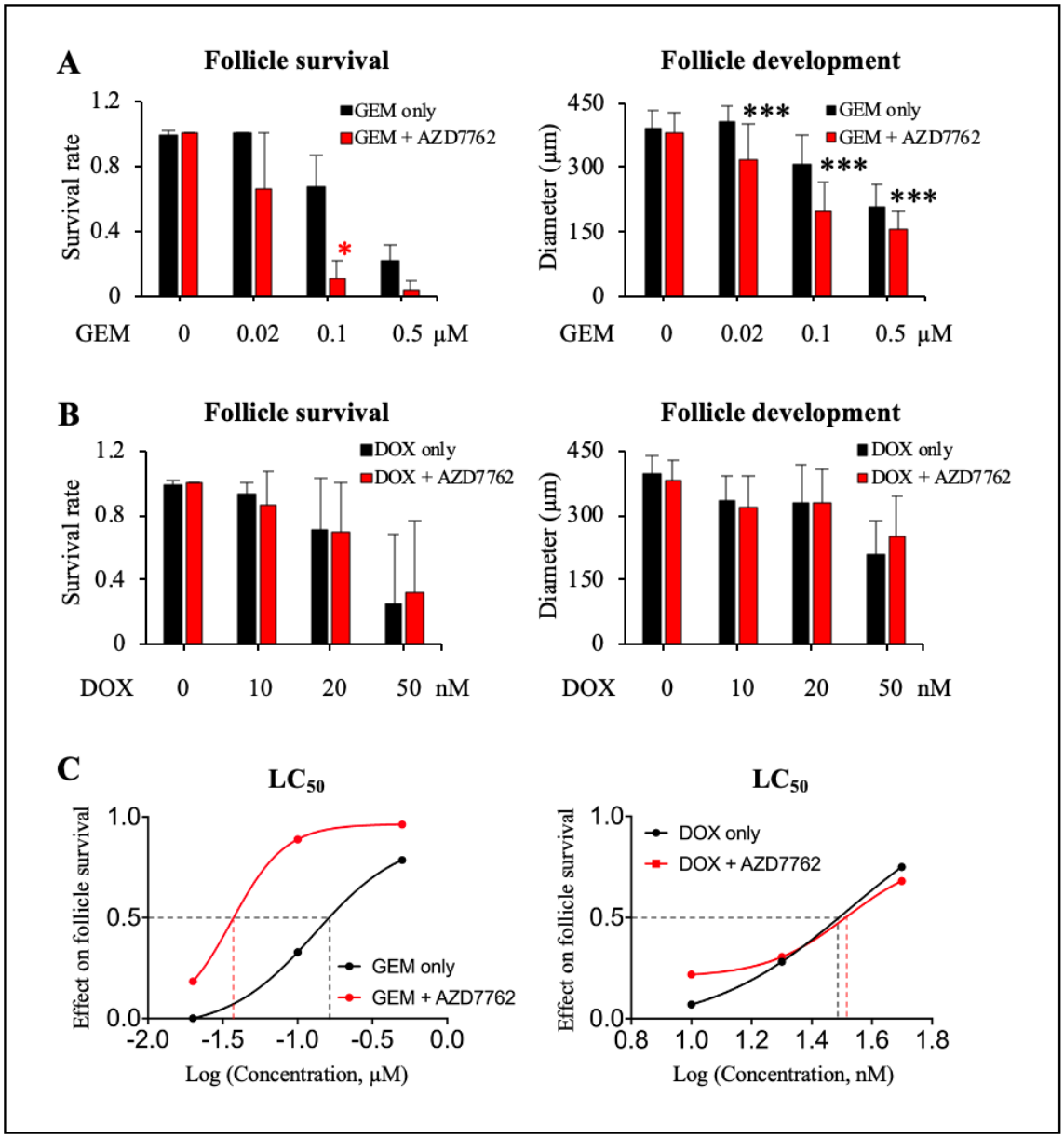

Figure 3.9 Effect of AZD7762 on exacerbating chemotherapeutic chemical-induced ovotoxicity. (A-B) Follicle survival rates and terminal diameters on day 8 of eIVFG after follicles were treated with gemcitabine (GEM) at 0, 0.02, 0.1 and 0.5 μM (A) or doxorubicin (DOX) at 0, 10, 20, and 50 nM (B) alone or co-treated with AZD7762 at 0.1 μM. (C) Effect of different doses of chemicals on follicle survival and LC_{50} value for log of concentration. Error bar: standard deviation; *$p<0.05$ and ***$p<0.001$ compared to control group. N=8-10 follicles in each experimental group and three replicates were performed.

CHAPTER 4

DISCUSSION

Ovotoxicity is one of the major off-target effects of pharmaceutical compounds. Previous studies have revealed that multiple drugs, such as chemotherapeutics, can damage ovarian follicles and increase the risk of premature ovarian failure, early menopause, and infertility in both reproductive aged women and prepubertal girls (Spears et al., 2019). The current gold standard for ovotoxicity testing relies on whole laboratory animals. However, it is challenging to use *in vivo* models to examine the specific and dynamic follicle and oocyte reproductive outcomes without dissecting whole animals, and it is also not feasible to use *in vivo* models to screen for the ovotoxicity of all hundreds of even thousands of candidate compounds. Tiered screening strategies have been increasingly employed in toxicity testing (Becker et al., 2007; Bus & Becker, 2009; Doe et al., 2006; Krewski et al., 2010). Compared to traditional methods using whole animals, the tiered screening is more efficient and cost-effective to identify and prioritize chemicals of low or high toxicity concern for the following more targeted and sophisticated assessments.

Previous studies have demonstrated that *in vitro* ovarian follicle culture is a robust model for ovotoxicity testing (Rasmussen et al., 2017; Stefansdottir et al., 2014; Wang et al., 2018; Xiao, Duncan, et al., 2015; Xiao, Zhang, et al., 2017a; Zhou & Flaws, 2017; Zhou et al., 2015; Zhou & Shikanov, 2018). Here, we developed a tiered ovotoxicity screening approach to identify pharmaceutical compounds of high ovotoxicity concern.

The tiered screening begins with eIVFG in Tier 1, a 3D *in vitro* follicle growth method we have previously developed (Xiao, Duncan, et al., 2015; Xiao, Zhang, et al., 2015; Xiao, Zhang, et al., 2017b), as a highly sensitive but less sophisticated screening method. If the tested compounds present negative ovotoxicities, they will be considered as low ovotoxicity concern. In contrast, for compounds that do not pass Tier 1 screening, more complex approaches will be used to further determine the likelihood and extent of the potential ovotoxicity in the Tier 2 and 3 screenings. In addition, the results obtained in Tier 1 will also be used to determine which specific tests should be conducted in Tier 2 and 3.

Our Tier 1 screening results showed that all the tested AZ compounds except AZD7762 (AZ-H) had no impact on the follicle and oocyte health (Figure 3.2-4). However, AZD7762 is a suspect ovotoxic chemical. In Tier 2, we chose AZD7762 with suspicious ovotoxicity and AZD8542 with negative ovotoxicity for a more sophisticated dose-response study and obtained consistent ovotoxic results (Figure 3.5-6). Specifically, we found that AZD7762 primarily damages granulosa cells but not oocytes to induce the entire follicle atresia (Figure 3.7A). Furthermore, we validated the positive and negative ovotoxicities of AZD7762 and AZD8542, respectively, using *in vivo* animal models in Tier 3 (Figure 3.8). These results suggest that eIVFG has a great potential to serve as an effective and efficient *in vitro* model for identifying and prioritizing chemicals of high ovotoxicity concern.

AZD7762 was originally designed as a selective ATP-competitive Chk1 inhibitor to abrogate S or G2 phase checkpoints to enhance DNA-damaging agent-induced cancer cell death, particularly for cancer cells that are deficient in the G1-DNA damage

checkpoint due to *Tp53* mutation (Zabludoff et al., 2008). It was later found that AZD7762 also had an equal inhibiting potency on Chk2 (Ma et al., 2011; Morgan et al., 2010; L. Wang et al., 2018; Zabludoff et al., 2008). Chk1 and Chk2 are serine/threonine specific protein kinases and coordinate DNA damage response (DDR). When DNA damage occurs during mitosis or upon genotoxic insults, ataxia telangiectasia-mutated (ATM) and/or ATM and Rad3-related (ATR) are phosphorylated and activated (Abraham, 2001; Yang et al., 2003), which in turn activate Chk2 and Chk1 through phosphorylation (Reinhardt & Yaffe, 2009; Smith et al., 2010), respectively. The activated ATM/Chk2 and/or ATR/Chk1 pathways further lead to Cdk1/2 inhibition through Chk1/Chk2-dependent phosphorylation and degradation of Cdc25 (Falck et al., 2001; Goto et al., 2019; Thanasoula et al., 2012), triggering cell cycle arrest and DNA repair to maintain DNA integrity. When the DNA damage is too much and irreparable, the cells undergo apoptosis (Zhang & Hunter, 2014). The dose-response results from Tier 2 indicated that AZD7762 at 1 and 10 μM severely promoted granulosa cell apoptosis (Figure 3.5 and 7). Previous studies demonstrated that global deletion of Chk2 does not impair female mouse fertility (Bolcun-Filas et al., 2014; Hirao et al., 2002; Takai et al., 2002). Moreover, our results indicated that BML-277, a specific checkpoint kinase inhibitor targeting Chk2 but not Chk1 (Arienti et al., 2005), was not ovotoxic (Figure 3.7B and 7C), suggesting that the AZD7762-induced granulosa cell apoptosis was not directly caused by its inhibitory effect on Chk2.

There is limited data regarding the role of Chk1 in ovarian follicle development and survival because Chk1-deficiency is embryonically lethal during the peri-implantation period (Liu et al., 2000; Takai et al., 2000). To determine whether the

AZD7762-induced follicle death is caused by Chk1 inhibition, we tested three Chk1-specific inhibitors and found that all three Chk1 inhibitors showed consistent ovotoxicities to AZD7762 (Figure 3.7B and 7C), indicating that inhibition of Chk1 may play essential roles in AZD7762-induced granulosa cell death. Since granulosa cells are mitotically active during folliculogenesis, we speculate that the inhibition of Chk1 and subsequent lack of Chk1-mediated cell cycle arrest and DNA repair, upon AZD7762 or other Chk1 inhibitor treatment, result in excessive accumulation of DNA damage, which triggers granulosa cell apoptosis. Chk1 has also been reported to regulate cell cycle transition during normal mitotic division, such as the G1/S transition, S phase progression, mitotic entry, and mitosis (Patil et al., 2013; Zhang & Hunter, 2014). As granulosa cells are actively proliferating during folliculogenesis (Lu et al., 2005), it is therefore also possible that the inhibition of Chk1 disrupts cell cycle transition during granulosa cell proliferation, leading to apoptosis and the subsequent entire follicle atresia. However, the underlying molecular mechanism of Chk1 inhibition and granulosa cell apoptosis requires further investigations.

In addition to inhibiting Chk1, it is also possible that the granulosa cell apoptosis induced by AZD7762 or other Chk1 inhibitors is caused by other off-target effects. For example, rabusertib, a specific Chk1 inhibitor, has been found to not only inhibit the phosphorylation of Chk1 at Ser296, the major mechanism to potentiate DNA damaging agent-induced cancer cell death, but also directly result in cancer cell DNA damage and apoptosis (van Harten et al., 2019; Wang et al., 2014). Moreover, although two Phase I clinical trials demonstrated that AZD7762 could enhance the anticancer effect of two widely used therapeutic chemicals, GEM and irinotecan (Ho et al., 2011; Sausville et al.,

2014), it was not advanced to Phase II stage due to the unintended cardiotoxicity (Ho et al., 2011; Reichert et al., 2016; Sausville et al., 2014). It was hypothesized that AZD7762 may inhibit other non-checkpoint kinases or ATP-dependent non-kinase proteins to cause cytotoxicities in cardiomyocytes (Ma et al., 2011; Manic et al., 2015), because another Chk1 specific inhibitor, MK-8776, did not show cardiotoxicity (Daud et al., 2015). Taken together, these results indicate that further studies are necessary to elucidate the specific underlying molecular mechanism of Chk1 inhibitor-induced ovotoxicities. Transgenic mice with conditional deletion of Chk1 in granulosa cells will help to confirm the role of Chk1 in granulosa cell survival and proliferation.

GEM has been demonstrated to induce cancer cell DNA damage and activate Chk1 but not Chk2 through phosphorylation (Isono et al., 2017; Morgan et al., 2006). Activated Chk1 further phosphorylates Cdc25A to induce its proteolytic degradation and results in CDK2 deactivation and cell cycle arrest at the S or G2 phase to allow for DNA damage repair (Patil et al., 2013; Zhang & Hunter, 2014). When the levels of GEM-induced DNA damage are too high to be fully repaired, cancer cells undergo apoptosis. It has been well demonstrated that co-treatment with AZD7762 abrogated Chk1-mediated cell cycle arrest and potentiated GEM-induced cancer cell apoptosis (Isono et al., 2017; Landau et al., 2012; Liu et al., 2017). For non-cancerous cells, it was expected that there is a functional G1 checkpoint pathway allowing for DNA damage repair and cell survival (Abraham, 2001; Zhang & Hunter, 2014), thus the co-treatment with AZD7762 will only or primarily potentiate the cytotoxicities of DNA damaging agents on cancer cells (Zabludoff et al., 2008). However, our results revealed that although AZD7762 at 0.1 μM alone did not induce follicle atresia as the higher concentrations at 1 and 10 μM did, the

co-treatment with AZD7762 at 0.1 μM significantly enhanced GEM-induced growing follicle death (Figure 3.9). These results suggest that the exacerbating effect of AZD7762 on GEM's ovotoxicities might be primarily induced by inhibiting Chk1-mediated cell cycle arrest and DNA repair. Interestingly, with respect to DOX which has been found to damage growing follicles through inducing granulosa cell apoptosis (Xiao, Zhang, et al., 2017a), the co-treatment with AZD7762 did not show any exacerbating effect (Figure 3.9). These results suggest that unlike the GEM-induced DNA damage and Chk1-mediated cell cycle arrest or cell apoptosis, DOX may use different molecular mechanisms to promote granulosa cell apoptosis in growing follicles.

The *in vivo* animal models in Tier 3 demonstrated that the clinically relevant exposure level of AZD7762 promoted the death of growing follicles but not primordial follicles (Figure 3.8), indicating that the dormant state of primordial follicles, particular the mitotically inactive pregranulosa cells, are less sensitive to AZD7762. Similarly, previous studies also found that several chemotherapeutic chemicals, such as cyclophosphamide, primarily damaged growing follicles but not primordial follicles, and the depletion or reduction of growing follicles could in turn overactivate primordial follicles, exhausting the ovarian reserve (Gonfloni et al., 2009; Kim et al., 2013; Kim et al., 2018; Nguyen et al., 2018). Therefore, although AZD7762 did not directly affect primordial follicle survival, its damaging effect on growing follicles will also increase the risk of premature ovarian failure, early menopause, and infertility through overactivating primordial follicles and diminishing the ovarian reserve.

One of the limitations of our current study is that there is no liver metabolism in the eIVFG system. However, some chemicals may require liver metabolic activation to

exhibit ovotoxicity or liver detoxification may inactivate the parent compound which is ovotoxic. To resolve this issue, one potential approach is to include the metabolite(s) in addition to the parental compound for *in vitro* compound exposure. A more encouraging approach is to use the emerging microfluidic technology to interconnect *in vitro* cultured ovarian tissues with liver organoids or cell lines to incorporate a more *in vivo*-like liver metabolism and pharmacokinetics into ovotoxicity testing. For example, we recently created a microfluidic platform that can integrate 2 or 5 different tissues together to study the tissue-tissue communications (Xiao, Coppeta, et al., 2017). However, its high cost and low-throughput properties limit its application in high-throughput ovotoxicity screening, which requires further improvement. Another limitation here is that eIVFG supports follicle growth starting from the primary or secondary stage. However, due to the technical difficulties, it is challenging to individually culture primordial follicles *in vitro*. Previous studies have cultured mouse neonatal whole ovaries or ovarian explants (Kim et al., 2013), which is a good model to study the impact of pharmaceutical compounds on primordial follicle survival and activation. Comparing to the *in vivo* model, eIVFG is difficult to detect the ovotoxity of life-span exposure because we only cultured the follicles for several days in a specific exposure window. For example, one study found that the carcinogenic effects of aspartame are increased using the *in vivo* model when the rats had a life-span exposure which begins during fetal life (Soffritti et al., 2007).

In summary, our study demonstrates that eIVFG is a robust *in vitro* model for testing the effects of pharmaceutical compounds on female ovarian functions and fertility. The developed tiered ovotoxicity screening can efficiently and effectively help us

identify and prioritize candidate compounds of high ovotoxicity concern for subsequent more targeted, sophisticated, and mechanistic *in vitro* and *in vivo* ovotoxicity assessments. In additional to pharmaceutical compounds, the developed tiered ovotoxicity screening method also provides good models for investigating the impact of environmental contaminants on female ovarian functions and fertility.

REFERENCES

Abraham, R. T. (2001). Cell cycle checkpoint signaling through the ATM and ATR kinases. *Genes & Development, 15*(17), 2177-2196. doi:DOI 10.1101/gad.914401

Arienti, K. L., Brunmark, A., Axe, F. U., McClure, K., Lee, A., Blevitt, J., . . . Breitenbucher, J. G. (2005). Checkpoint kinase inhibitors: SAR and radioprotective properties of a series of 2-arylbenzimidazoles. *J Med Chem, 48*(6), 1873-1885. doi:10.1021/jm0495935

Bakke, O. M., Manocchia, M., Deabajo, F., Kaitin, K. I., & Lasagna, L. (1995). Drug Safety Discontinuations in the United-Kingdom, the United-States, and Spain from 1974 through 1993 - a Regulatory Perspective. *Clinical Pharmacology & Therapeutics, 58*(1), 108-117. doi:Doi 10.1016/0009-9236(95)90078-0

Becker, R. A., Plunkett, L. M., Borzelleca, J. F., & Kaplan, A. M. (2007). Tiered toxicity testing: evaluation of toxicity-based decision triggers for human health hazard characterization. *Food Chem Toxicol, 45*(12), 2454-2469. doi:10.1016/j.fct.2007.05.030

Ben-Aharon, I., Bar-Joseph, H., Tzarfaty, G., Kuchinsky, L., Rizel, S., Stemmer, S. M., & Shalgi, R. (2010). Doxorubicin-induced ovarian toxicity. *Reprod Biol Endocrinol, 8*, 20. doi:10.1186/1477-7827-8-20

Bhattacharya, P., & Keating, A. F. (2012). Impact of environmental exposures on ovarian function and role of xenobiotic metabolism during ovotoxicity. *Toxicol Appl Pharmacol, 261*(3), 227-235. doi:10.1016/j.taap.2012.04.009

Biggers, J. D., Whittingham, D. G., & Donahue, R. P. (1967). The pattern of energy metabolism in the mouse oocyte and zygote. *Proc Natl Acad Sci U S A, 58*(2), 560-567.

Bolcun-Filas, E., Rinaldi, V. D., White, M. E., & Schimenti, J. C. (2014). Reversal of female infertility by Chk2 ablation reveals the oocyte DNA damage checkpoint pathway. *Science, 343*(6170), 533-536. doi:10.1126/science.1247671

Boudny, M., Zemanova, J., Khirsariya, P., Borsky, M., Verner, J., Cerna, J., . . . Trbusek, M. (2019). Novel CHK1 inhibitor MU380 exhibits significant single-agent activity in TP53-mutated chronic lymphocytic leukemia cells. *Haematologica, 104*(12), 2443-2455. doi:10.3324/haematol.2018.203430

Buccione, R., Schroeder, A. C., & Eppig, J. J. (1990). Interactions between Somatic-Cells and Germ-Cells Throughout Mammalian Oogenesis. *Biology of Reproduction, 43*(4), 543-547. doi:Doi 10.1095/Biolreprod43.4.543

Bus, J. S., & Becker, R. A. (2009). Toxicity testing in the 21st century: a view from the chemical industry. *Toxicol Sci, 112*(2), 297-302. doi:10.1093/toxsci/kfp234

Buyuk, E., Nejat, E., & Neal-Perry, G. (2010). Determinants of female reproductive senescence: differential roles for the ovary and the neuroendocrine axis. *Semin Reprod Med, 28*(5), 370-379. doi:10.1055/s-0030-1262896

Chen, J., Torcia, S., Xie, F., Lin, C. J., Cakmak, H., Franciosi, F., . . . Conti, M. (2013). Somatic cells regulate maternal mRNA translation and developmental competence of mouse oocytes. *Nat Cell Biol, 15*(12), 1415-1423. doi:10.1038/ncb2873

Dai, B. J., Zhao, X. F., Mazan-Mamczarz, K., Hagner, P., Corl, S., Bahassi, E. M., . . . Gartenhaus, R. B. (2011). Functional and molecular interactions between ERK and CHK2 in diffuse large B-cell lymphoma. *Nature Communications, 2*. doi:ARTN 40210.1038/ncomms1404

Daud, A. I., Ashworth, M. T., Strosberg, J., Goldman, J. W., Mendelson, D., Springett, G., . . . Munster, P. N. (2015). Phase I dose-escalation trial of checkpoint kinase 1 inhibitor MK-8776 as monotherapy and in combination with gemcitabine in patients with advanced solid tumors. *Journal of Clinical Oncology, 33*(9), 1060-1066. doi:10.1200/JCO.2014.57.5027

DiMasi, J. A., Grabowski, H. G., & Hansen, R. W. (2016). Innovation in the pharmaceutical industry: New estimates of R&D costs. *J Health Econ, 47*, 20-33. doi:10.1016/j.jhealeco.2016.01.012

Doe, J. E., Boobis, A. R., Blacker, A., Dellarco, V., Doerrer, N. G., Franklin, C., . . . Wolf, D. C. (2006). A tiered approach to systemic toxicity testing for agricultural chemical safety assessment. *Crit Rev Toxicol, 36*(1), 37-68. doi:10.1080/10408440500534370

Eisenstein, E. L., Lemons, P. W., 2nd, Tardiff, B. E., Schulman, K. A., Jolly, M. K., & Califf, R. M. (2005). Reducing the costs of phase III cardiovascular clinical trials. *Am Heart J, 149*(3), 482-488. doi:10.1016/j.ahj.2004.04.049

Eppig, J. J., Pendola, F. L., Wigglesworth, K., & Pendola, J. K. (2005). Mouse oocytes regulate metabolic cooperativity between granulosa cells and oocytes: amino acid transport. *Biology of Reproduction, 73*(2), 351-357. doi:10.1095/biolreprod.105.041798

Falck, J., Mailand, N., Syljuasen, R. G., Bartek, J., & Lukas, J. (2001). The ATM-Chk2-Cdc25A checkpoint pathway guards against radioresistant DNA synthesis. *Nature, 410*(6830), 842-847. doi:10.1038/35071124

FDA. (2017). S5(R3)Detection of Toxicity to Reproduction. Retrieved from https://www.fda.gov

Gilchrist, R. B., Ritter, L. J., Myllymaa, S., Kaivo-Oja, N., Dragovic, R. A., Hickey, T. E., . . . Mottershead, D. G. (2006). Molecular basis of oocyte-paracrine signalling that promotes granulosa cell proliferation. *J Cell Sci, 119*(Pt 18), 3811-3821. doi:10.1242/jcs.03105

Gonfloni, S., Di Tella, L., Caldarola, S., Cannata, S. M., Klinger, F. G., Di Bartolomeo, C., . . . Cesareni, G. (2009). Inhibition of the c-Abl-TAp63 pathway protects mouse oocytes from chemotherapy-induced death. *Nat Med, 15*(10), 1179-1185. doi:10.1038/nm.2033

Goto, H., Natsume, T., Kanemaki, M. T., Kaito, A., Wang, S. J., Gabazza, E. C., . . . Mizoguchi, A. (2019). Chk1-mediated Cdc25A degradation as a critical mechanism for normal cell cycle progression. *Journal of Cell Science, 132*(2). doi:UNSP jcs22312310.1242/jcs.223123

Gui, U. M., & Joyce, L. A. (2005). RNA interference evidence that growth differentiation factor-9 mediates clocyte regulation of cumulus expansion in mice. *Biology of Reproduction, 72*(1), 195-199. doi:Doi 10.1095/Biolreprod.104.033357

Gynecologists, T. A. C. o. O. a. (2015). Ethical Considerations for Including Women as Research Participants. Retrieved from https://www.acog.org

Havelock, J. C., Rainey, W. E., & Carr, B. R. (2004). Ovarian granulosa cell lines. *Mol Cell Endocrinol, 228*(1-2), 67-78. doi:10.1016/j.mce.2004.04.018

Hirao, A., Cheung, A., Duncan, G., Girard, P. M., Elia, A. J., Wakeham, A., . . . Mak, T. W. (2002). Chk2 is a tumor suppressor that regulates apoptosis in both an ataxia telangiectasia mutated (ATM)-dependent and an ATM-independent manner. *Molecular and Cellular Biology, 22*(18), 6521-6532. doi:10.1128/Mcb.22.18.6521-6532.2002

Ho, A. L., Bendell, J. C., Cleary, J. M., Schwartz, G. K., Burris, H. A., Oakes, P., . . . Shapiro, G. (2011). Phase I, open-label, dose-escalation study of AZD7762 in combination with irinotecan (irino) in patients (pts) with advanced solid tumors. *Journal of Clinical Oncology, 29*(15).

Hwang, R. F., Moore, T. T., Hattersley, M. M., Scarpitti, M., Yang, B., Devereaux, E., . . . Godin, R. (2012). Inhibition of the Hedgehog Pathway Targets the Tumor-Associated Stroma in Pancreatic Cancer. *Molecular Cancer Research, 10*(9), 1147-1157. doi:10.1158/1541-7786.Mcr-12-0022

Isono, M., Hoffmann, M. J., Pinkerneil, M., Sato, A., Michaelis, M., Cinatl, J., . . . Schulz, W. A. (2017). Checkpoint kinase inhibitor AZD7762 strongly sensitises urothelial carcinoma cells to gemcitabine. *Journal of Experimental & Clinical Cancer Research, 36*. doi:ARTN 110.1186/s13046-016-0473-1

Itamochi, H., Nishimura, M., Oumi, N., Kato, M., Oishi, T., Shimada, M., . . . Harada, T. (2014). Checkpoint kinase inhibitor AZD7762 overcomes cisplatin resistance in clear cell carcinoma of the ovary. *Int J Gynecol Cancer, 24*(1), 61-69. doi:10.1097/IGC.0000000000000014

Karp, J. E., Thomas, B. M., Greer, J. M., Sorge, C., Gore, S. D., Pratz, K. W., . . . Kaufmann, S. H. (2012). Phase I and pharmacologic trial of cytosine arabinoside with the selective checkpoint 1 inhibitor Sch 900776 in refractory acute leukemias. *Clin Cancer Res, 18*(24), 6723-6731. doi:10.1158/1078-0432.CCR-12-2442

Keren-Tal, I., Dantes, A., Sprengel, R., & Amsterdam, A. (1993). Establishment of steroidogenic granulosa cell lines expressing follicle stimulating hormone receptors. *Mol Cell Endocrinol, 95*(1-2), R1-10. doi:10.1016/0303-7207(93)90042-i

Kim, S. Y., Cordeiro, M. H., Serna, V. A., Ebbert, K., Butler, L. M., Sinha, S., . . . Kurita, T. (2013). Rescue of platinum-damaged oocytes from programmed cell death through inactivation of the p53 family signaling network. *Cell Death and Differentiation, 20*(8), 987-997. doi:10.1038/cdd.2013.31

Kim, S. Y., Nair, D. M., Romero, M., Serna, V. A., Koleske, A. J., Woodruff, T. K., & Kurita, T. (2018). Transient inhibition of p53 homologs protects ovarian function from two distinct apoptotic pathways triggered by anticancer therapies. *Cell Death and Differentiation*. doi:10.1038/s41418-018-0151-2

King, C., Diaz, H., Barnard, D., Barda, D., Clawson, D., Blosser, W., . . . Marshall, M. (2014). Characterization and preclinical development of LY2603618: a selective and potent Chk1 inhibitor. *Invest New Drugs, 32*(2), 213-226. doi:10.1007/s10637-013-0036-7

Kreeger, P. K., Deck, J. W., Woodruff, T. K., & Shea, L. D. (2006). The in vitro regulation of ovarian follicle development using alginate-extracellular matrix gels. *Biomaterials, 27*(5), 714-723. doi:10.1016/j.biomaterials.2005.06.016

Kreeger, P. K., Fernandes, N. N., Woodruff, T. K., & Shea, L. D. (2005). Regulation of mouse follicle development by follicle-stimulating hormone in a three-dimensional in vitro culture system is dependent on follicle stage and dose. *Biol Reprod, 73*(5), 942-950. doi:10.1095/biolreprod.105.042390

Krewski, D., Acosta, D., Jr., Andersen, M., Anderson, H., Bailar, J. C., 3rd, Boekelheide, K., . . . Zeise, L. (2010). Toxicity testing in the 21st century: a vision and a strategy. *J Toxicol Environ Health B Crit Rev, 13*(2-4), 51-138. doi:10.1080/10937404.2010.483176

Landau, H. J., McNeely, S. C., Nair, J. S., Comenzo, R. L., Asai, T., Friedman, H., . . . Schwartz, G. K. (2012). The checkpoint kinase inhibitor AZD7762 potentiates chemotherapy-induced apoptosis of p53-mutated multiple myeloma cells. *Molecular Cancer Therapeutics, 11*(8), 1781-1788. doi:10.1158/1535-7163.MCT-11-0949

Liu, Q. H., Guntuku, S., Cui, X. S., Matsuoka, S., Cortez, D., Tamai, K., . . . Elledge, S. J. (2000). Chk1 is an essential kinase that is regulated by Atr and required for the G(2)/M DNA damage checkpoint. *Genes & Development, 14*(12), 1448-1459.

Liu, Y., Li, Y., Wang, X., Liu, F., Gao, P., Quinn, M. M., . . . Wong, K. K. (2017). Gemcitabine and Chk1 Inhibitor AZD7762 Synergistically Suppress the Growth of Lkb1-Deficient Lung Adenocarcinoma. *Cancer Res, 77*(18), 5068-5076. doi:10.1158/0008-5472.CAN-17-0567

Lu, C. L., Yang, W., Hu, Z. Y., & Liu, Y. X. (2005). Granulosa cell proliferation differentiation and its role in follicular development. *Chinese Science Bulletin, 50*(23), 2665-2671. doi:10.1360/982005-983

Ma, C. X., Janetka, J. W., & Piwnica-Worms, H. (2011). Death by releasing the breaks: CHK1 inhibitors as cancer therapeutics. *Trends Mol Med, 17*(2), 88-96. doi:10.1016/j.molmed.2010.10.009

Ma, Z., Yao, G., Zhou, B., Fan, Y., Gao, S., & Feng, X. (2012). The Chk1 inhibitor AZD7762 sensitises p53 mutant breast cancer cells to radiation in vitro and in vivo. *Mol Med Rep, 6*(4), 897-903. doi:10.3892/mmr.2012.999

Manic, G., Obrist, F., Sistigu, A., & Vitale, I. (2015). Trial Watch: Targeting ATM-CHK2 and ATR-CHK1 pathways for anticancer therapy. *Mol Cell Oncol, 2*(4), e1012976. doi:10.1080/23723556.2015.1012976

Matzuk, M. M., Burns, K. H., Viveiros, M. M., & Eppig, J. J. (2002). Intercellular communication in the mammalian ovary: oocytes carry the conversation. *Science, 296*(5576), 2178-2180. doi:10.1126/science.1071965

Morgan, M. A., Parsels, L. A., Parsels, J. D., Lawrence, T. S., & Maybaum, J. (2006). The relationship of premature mitosis to cytotoxicity in response to checkpoint abrogation and antimetabolite treatment. *Cell Cycle, 5*(17), 1983-1988. doi:10.4161/cc.5.17.3184

Morgan, M. A., Parsels, L. A., Zhao, L., Parsels, J. D., Davis, M. A., Hassan, M. C., . . . Lawrence, T. S. (2010). Mechanism of radiosensitization by the Chk1/2 inhibitor AZD7762 involves abrogation of the G2 checkpoint and inhibition of homologous recombinational DNA repair. *Cancer Res, 70*(12), 4972-4981. doi:10.1158/0008-5472.CAN-09-3573

Nguyen, Q. N., Zerafa, N., Liew, S. H., Morgan, F. H., Strasser, A., Scott, C. L., . . . Hutt, K. J. (2018). Loss of PUMA protects the ovarian reserve during DNA-damaging chemotherapy and preserves fertility. *Cell Death Dis, 9*(6), 618. doi:10.1038/s41419-018-0633-7

Onakpoya, I. J., Heneghan, C. J., & Aronson, J. K. (2016). Post-marketing withdrawal of 462 medicinal products because of adverse drug reactions: a systematic review of the world literature. *BMC Med, 14*, 10. doi:10.1186/s12916-016-0553-2

Patil, M., Pabla, N., & Dong, Z. (2013). Checkpoint kinase 1 in DNA damage response and cell cycle regulation. *Cellular and Molecular Life Sciences, 70*(21), 4009-4021. doi:10.1007/s00018-013-1307-3

Pocar, P., Augustin, R., Gandolfi, F., & Fischer, B. (2003). Toxic effects of in vitro exposure to p-tert-octylphenol on bovine oocyte maturation and developmental competence. *Biology of Reproduction, 69*(2), 462-468. doi:10.1095/biolreprod.102.010355

Pocar, P., Perazzoli, F., Luciano, A. M., & Gandolfi, F. (2001). In vitro reproductive toxicity of polychlorinated biphenyls: effects on oocyte maturation and developmental competence in cattle. *Mol Reprod Dev, 58*(4), 411-416. doi:10.1002/1098-2795(20010401)58:4<411::AID-MRD8>3.0.CO;2-R

Quin, J., Chan, K. T., Devlin, J. R., Cameron, D. P., Diesch, J., Cullinane, C., . . . Hannan, R. D. (2016). Inhibition of RNA polymerase I transcription initiation by CX-5461 activates non-canonical ATM/ATR signaling. *Oncotarget, 7*(31), 49800-49818. doi:10.18632/oncotarget.10452

Rasmussen, L. M., Sen, N., Vera, J. C., Liu, X., & Craig, Z. R. (2017). Effects of in vitro exposure to dibutyl phthalate, mono-butyl phthalate, and acetyl tributyl citrate on ovarian antral follicle growth and viability. *Biol Reprod, 96*(5), 1105-1117. doi:10.1095/biolreprod.116.144691

Reichert, Z. R., Wahl, D. R., & Morgan, M. A. (2016). Translation of Targeted Radiation Sensitizers into Clinical Trials. *Seminars in Radiation Oncology, 26*(4), 261-270. doi:10.1016/j.semradonc.2016.06.001

Reinhardt, H. C., & Yaffe, M. B. (2009). Kinases that control the cell cycle in response to DNA damage: Chk1, Chk2, and MK2. *Current Opinion in Cell Biology, 21*(2), 245-255. doi:10.1016/j.ceb.2009.01.018

Roti Roti, E. C., Leisman, S. K., Abbott, D. H., & Salih, S. M. (2012). Acute doxorubicin insult in the mouse ovary is cell- and follicle-type dependent. *PloS one, 7*(8), e42293. doi:10.1371/journal.pone.0042293

Sausville, E., Lorusso, P., Carducci, M., Carter, J., Quinn, M. F., Malburg, L., . . . Senderowicz, A. (2014). Phase I dose-escalation study of AZD7762, a checkpoint kinase inhibitor, in combination with gemcitabine in US patients with advanced solid tumors. *Cancer Chemother Pharmacol, 73*(3), 539-549. doi:10.1007/s00280-014-2380-5

Seto, T., Esaki, T., Hirai, F., Arita, S., Nosaki, K., Makiyama, A., . . . Shi, X. (2013). Phase I, dose-escalation study of AZD7762 alone and in combination with gemcitabine in Japanese patients with advanced solid tumours. *Cancer Chemother Pharmacol, 72*(3), 619-627. doi:10.1007/s00280-013-2234-6

Siramshetty, V. B., Nickel, J., Omieczynski, C., Gohlke, B. O., Drwal, M. N., & Preissner, R. (2016). WITHDRAWN--a resource for withdrawn and discontinued drugs. *Nucleic Acids Res, 44*(D1), D1080-1086. doi:10.1093/nar/gkv1192

Smith, J., Tho, L. M., Xu, N. H., & Gillespie, D. A. (2010). The ATM-Chk2 and ATR-Chk1 Pathways in DNA Damage Signaling and Cancer. *Advances in Cancer Research, Vol 108, 108*, 73-112. doi:10.1016/S0065.230x(10)08002.4

Soffritti, M., Belpoggi, F., Tibaldi, E., Esposti, D. D., & Lauriola, M. (2007). Life-span exposure to low doses of aspartame beginning during prenatal life increases cancer effects in rats. *Environ Health Perspect, 115*(9), 1293-1297. doi:10.1289/ehp.10271

Songsasen, N., Woodruff, T. K., & Wildt, D. E. (2011). In vitro growth and steroidogenesis of dog follicles are influenced by the physical and hormonal microenvironment. *Reproduction, 142*(1), 113-122. doi:10.1530/REP-10-0442

Spears, N., Lopes, F., Stefansdottir, A., Rossi, V., De Felici, M., Anderson, R. A., & Klinger, F. G. (2019). Ovarian damage from chemotherapy and current approaches to its protection. *Hum Reprod Update, 25*(6), 673-693. doi:10.1093/humupd/dmz027

Stefansdottir, A., Fowler, P. A., Powles-Glover, N., Anderson, R. A., & Spears, N. (2014). Use of ovary culture techniques in reproductive toxicology. *Reprod Toxicol, 49*, 117-135. doi:10.1016/j.reprotox.2014.08.001

Su, Y. Q., Sugiura, K., & Eppig, J. J. (2009). Mouse oocyte control of granulosa cell development and function: paracrine regulation of cumulus cell metabolism. *Semin Reprod Med, 27*(1), 32-42. doi:10.1055/s-0028-1108008

Su, Y. Q., Sugiura, K., Wigglesworth, K., O'Brien, M. J., Affourtit, J. P., Pangas, S. A., . . . Eppig, J. J. (2008). Oocyte regulation of metabolic cooperativity between mouse cumulus cells and oocytes: BMP15 and GDF9 control cholesterol biosynthesis in cumulus cells. *Development, 135*(1), 111-121. doi:10.1242/dev.009068

Sugiura, K., Pendola, F. L., & Eppig, J. J. (2005). Oocyte control of metabolic cooperativity between oocytes and companion granulosa cells: energy metabolism. *Dev Biol, 279*(1), 20-30. doi:10.1016/j.ydbio.2004.11.027

Takai, H., Naka, K., Okada, Y., Watanabe, M., Harada, N., Saito, S., . . . Motoyama, N. (2002). Chk2-deficient mice exhibit radioresistance and defective p53-mediated transcription. *EMBO J, 21*(19), 5195-5205. doi:10.1093/emboj/cdf506

Takai, H., Tominaga, K., Motoyama, N., Minamishima, Y. A., Nagahama, H., Tsukiyama, T., . . . Nakayama, K. (2000). Aberrant cell cycle checkpoint function and early embryonic death in Chk1(-/-) mice. *Genes & Development, 14*(12), 1439-1447.

Thanasoula, M., Escandell, J. M., Suwaki, N., & Tarsounas, M. (2012). ATM/ATR checkpoint activation downregulates CDC25C to prevent mitotic entry with uncapped telomeres. *Embo Journal, 31*(16), 3398-3410. doi:10.1038/emboj.2012.191

Tse, A. N., Rendahl, K. G., Sheikh, T., Cheema, H., Aardalen, K., Embry, M., . . . Schwartz, G. K. (2007). CHIR-124, a novel potent inhibitor of Chk1, potentiates the cytotoxicity of topoisomerase I poisons in vitro and in vivo. *Clin Cancer Res, 13*(2 Pt 1), 591-602. doi:10.1158/1078-0432.CCR-06-1424

Tuppi, M., Kehrloesser, S., Coutandin, D. W., Rossi, V., Luh, L. M., Strubel, A., . . . Dotsch, V. (2018). Oocyte DNA damage quality control requires consecutive interplay of CHK2 and CK1 to activate p63. *Nature Structural & Molecular Biology, 25*(3), 261-+. doi:10.1038/s41594-018-0035-7

Vabre, P., Gatimel, N., Moreau, J., Gayrard, V., Picard-Hagen, N., Parinaud, J., & Leandri, R. D. (2017). Environmental pollutants, a possible etiology for premature ovarian insufficiency: a narrative review of animal and human data. *Environ Health, 16*(1), 37. doi:10.1186/s12940-017-0242-4

van Harten, A. M., Buijze, M., van der Mast, R., Rooimans, M. A., Martens-de Kemp, S. R., Bachas, C., . . . Brakenhoff, R. H. (2019). Targeting the cell cycle in head and neck cancer by Chk1 inhibition: a novel concept of bimodal cell death. *Oncogenesis, 8*. doi:ARTN 3810.1038/s41389-019-0147-x

Wang, F. Z., Fei, H. R., Cui, Y. J., Sun, Y. K., Li, Z. M., Wang, X. Y., . . . Sun, B. L. (2014). The checkpoint 1 kinase inhibitor LY2603618 induces cell cycle arrest, DNA damage response and autophagy in cancer cells. *Apoptosis, 19*(9), 1389-1398. doi:10.1007/s10495-014-1010-3

Wang, L., Wang, Y., Chen, A., Jalali, A., Liu, S., Guo, Y., . . . Yokota, H. (2018). Effects of a checkpoint kinase inhibitor, AZD7762, on tumor suppression and bone remodeling. *Int J Oncol, 53*(3), 1001-1012. doi:10.3892/ijo.2018.4481

Wang, Y., Liu, M., Johnson, S. B., Yuan, G., Arriba, A. K., Zubizarreta, M. E., . . . Xiao, S. (2019a). Doxorubicin obliterates mouse ovarian reserve through both primordial follicle atresia and overactivation. *Toxicol Appl Pharmacol*, 114714. doi:10.1016/j.taap.2019.114714

Wang, Y., Liu, M., Johnson, S. B., Yuan, G., Arriba, A. K., Zubizarreta, M. E., . . . Xiao, S. (2019b). Doxorubicin obliterates mouse ovarian reserve through both primordial follicle atresia and overactivation. *Toxicol Appl Pharmacol, 381*, 114714. doi:10.1016/j.taap.2019.114714

Wang, Y., Liu, M., Zhang, J., Liu, Y., Kopp, M., Zheng, W., & Xiao, S. (2018). Multidrug Resistance Protein 1 Deficiency Promotes Doxorubicin-Induced Ovarian Toxicity in Female Mice. *Toxicol Sci, 163*(1), 279-292. doi:10.1093/toxsci/kfy038

Waring, M. J., Arrowsmith, J., Leach, A. R., Leeson, P. D., Mandrell, S., Owen, R. M., . . . Weir, A. (2015). An analysis of the attrition of drug candidates from four major pharmaceutical companies. *Nat Rev Drug Discov, 14*(7), 475-486. doi:10.1038/nrd4609

Wehler, T., Thomas, M., Schumann, C., Bosch-Barrera, J., Vinolas Segarra, N., Dickgreber, N. J., . . . Paz-Ares, L. (2017). A randomized, phase 2 evaluation of the CHK1 inhibitor, LY2603618, administered in combination with pemetrexed and cisplatin in patients with advanced nonsquamous non-small cell lung cancer. *Lung Cancer, 108*, 212-216. doi:10.1016/j.lungcan.2017.03.001

Wong, C. H., Siah, K. W., & Lo, A. W. (2019). Estimation of clinical trial success rates and related parameters. *Biostatistics, 20*(2), 273-286. doi:10.1093/biostatistics/kxx069

Wysowski, D. K., & Swartz, L. (2005). Adverse drug event surveillance and drug withdrawals in the United States, 1969-2002: the importance of reporting suspected reactions. *Arch Intern Med, 165*(12), 1363-1369. doi:10.1001/archinte.165.12.1363

Xiao, S., Coppeta, J. R., Rogers, H. B., Isenberg, B. C., Zhu, J., Olalekan, S. A., . . . Woodruff, T. K. (2017). A microfluidic culture model of the human reproductive tract and 28-day menstrual cycle. *Nat Commun, 8*, 14584. doi:10.1038/ncomms14584

Xiao, S., Duncan, F. E., Bai, L., Nguyen, C. T., Shea, L. D., & Woodruff, T. K. (2015). Size-specific follicle selection improves mouse oocyte reproductive outcomes. *Reproduction, 150*(3), 183-192. doi:10.1530/REP-15-0175

Xiao, S., Zhang, J., Liu, M., Iwahata, H., Rogers, H. B., & Woodruff, T. K. (2017a). Doxorubicin Has Dose-Dependent Toxicity on Mouse Ovarian Follicle Development, Hormone Secretion, and Oocyte Maturation. *Toxicol Sci, 157*(2), 320-329. doi:10.1093/toxsci/kfx047

Xiao, S., Zhang, J., Romero, M. M., Smith, K. N., Shea, L. D., & Woodruff, T. K. (2015). In vitro follicle growth supports human oocyte meiotic maturation. *Sci Rep, 5*, 17323. doi:10.1038/srep17323

Xiao, S., Zhang, J. Y., Liu, M. J., Iwahata, H., Rogers, H. B., & Woodruff, T. K. (2017b). Doxorubicin Has Dose-Dependent Toxicity on Mouse Ovarian Follicle Development, Hormone Secretion, and Oocyte Maturation. *Toxicological Sciences, 157*(2), 320-329. doi:10.1093/toxsci/kfx047

Xu, J., Lawson, M. S., Yeoman, R. R., Pau, K. Y., Barrett, S. L., Zelinski, M. B., & Stouffer, R. L. (2011). Secondary follicle growth and oocyte maturation during encapsulated three-dimensional culture in rhesus monkeys: effects of gonadotrophins, oxygen and fetuin. *Hum Reprod, 26*(5), 1061-1072. doi:10.1093/humrep/der049

Xu, M., Barrett, S. L., West-Farrell, E., Kondapalli, L. A., Kiesewetter, S. E., Shea, L. D., & Woodruff, T. K. (2009). In vitro grown human ovarian follicles from cancer patients support oocyte growth. *Hum Reprod, 24*(10), 2531-2540. doi:10.1093/humrep/dep228

Xu, M., Kreeger, P. K., Shea, L. D., & Woodruff, T. K. (2006). Tissue-engineered follicles produce live, fertile offspring. *Tissue Eng, 12*(10), 2739-2746. doi:10.1089/ten.2006.12.2739

Xu, M., West-Farrell, E. R., Stouffer, R. L., Shea, L. D., Woodruff, T. K., & Zelinski, M. B. (2009). Encapsulated three-dimensional culture supports development of nonhuman primate secondary follicles. *Biol Reprod, 81*(3), 587-594. doi:10.1095/biolreprod.108.074732

Yang, J., Yu, Y. N., Hamrick, H. E., & Duerksen-Hughes, P. J. (2003). ATM, ATR and DNA-PK: initiators of the cellular genotoxic stress responses. *Carcinogenesis, 24*(10), 1571-1580. doi:10.1093/carcin/bgg137

Yuksel, A., Bildik, G., Senbabaoglu, F., Akin, N., Arvas, M., Unal, F., . . . Oktem, O. (2015). The magnitude of gonadotoxicity of chemotherapy drugs on ovarian follicles and granulosa cells varies depending upon the category of the drugs and the type of granulosa cells. *Hum Reprod, 30*(12), 2926-2935. doi:10.1093/humrep/dev256

Zabludoff, S. D., Deng, C., Grondine, M. R., Sheehy, A. M., Ashwell, S., Caleb, B. L., . . . White, A. M. (2008). AZD7762, a novel checkpoint kinase inhibitor, drives checkpoint abrogation and potentiates DNA-targeted therapies. *Molecular Cancer Therapeutics, 7*(9), 2955-2966. doi:10.1158/1535-7163.MCT-08-0492

Zhang, Y., & Hunter, T. (2014). Roles of Chk1 in cell biology and cancer therapy. *Int J Cancer, 134*(5), 1013-1023. doi:10.1002/ijc.28226

Zhou, C., & Flaws, J. A. (2017). Effects of an Environmentally Relevant Phthalate Mixture on Cultured Mouse Antral Follicles. *Toxicol Sci, 156*(1), 217-229. doi:10.1093/toxsci/kfw245

Zhou, H., Malik, M. A., Arab, A., Hill, M. T., & Shikanov, A. (2015). Hydrogel Based 3-Dimensional (3D) System for Toxicity and High-Throughput (HTP) Analysis for Cultured Murine Ovarian Follicles. *PLoS One, 10*(10), e0140205. doi:10.1371/journal.pone.0140205

Zhou, H., & Shikanov, A. (2018). Three-Dimensional Hydrogel-Based Culture to Study the Effects of Toxicants on Ovarian Follicles. *Methods Mol Biol, 1758*, 55-72. doi:10.1007/978-1-4939-7741-3_5